Lee Jae Seong (Orcid ID: 0000-0002-9442-0676)
Lim Dhongil (Orcid ID: 0000-0002-0832-2907)
Kang Dong-Jin (Orcid ID: 0000-0001-5021-6502)

Sedimentary organic carbon budget across the slope to the basin in the southwestern Ulleung (Tsushima) Basin of the East (Japan) Sea

Jae Seong Lee[1,3,4*], Jeong Hee Han[5], Sung-Uk An[6], Sung-Han Kim[1], Dhongil Lim[2,3], Dongseon Kim[1,3,4], Dong-Jin Kang[1,3], Young–Kyu Park[1,3,4]

[1]Marine Environment Research Center, Korea Institute Ocean Science and Technology, Busan 49111, Korea
[2]Library of Marine Samples, South Sea Research Institute, Korea Institute of Ocean Science and Technology, Geoje 53201, South Korea
[3]Department of Integrated Ocean Sciences, Korea Institute Ocean Science and Technology campus of University of Science and Technology, Busan 49111, Korea
[4]Department of Convergence Study on the Ocean Science and Technology, Ocean Science and Technology Scholl, Busan 49111, Korea
[5]Earth and Environmental Research Center, Korea Basic Science Institute, Cheongju 28119, Korea
[6]Department of Marine Science and Convergence Engineering, Hanyang University, Ansan 15588, Korea

[*]Corresponding author: Jae Seong Lee (leejs@kiost.ac.kr)

- Competing interests statement

  Declaration of Interest: None.

- Authorship contribution statement

  Lee, J.S. (leejs@kiost.ac.kr): Conceptualization, Investigation, Benthic lander operation, Geochemical analysis, Writing-original draft. **Han, J.H. (hanjh@kbsi.re.kr):** Conceptualization, ^{210}Pb analysis. **An, S.-W. (asuppl@hanyang.ac.kr):** Investigation, Benthic lander operation, Geochemical analysis. **Kim, S.-H. (sunghan@kiost.ac.kr):** Conceptualization, Geochemical analysis, Writing-original draft. **Lim, D. (oceanlim@kiost.ac.kr):** Geochemical analysis, Writing-review. **Kim, D.-S. (dkim@kiost.ac.kr):** Conceptualization, Investigation, Writing-original draft. **Kang, D.-J. (djocean@kiost.ac.kr):** Investigation. **Park, Y.-K. (ypark@kiost.ac.kr):** Conceptualization.

Key Points:

- The sedimentary organic carbon mass budget was estimated in the southwestern part of Ulleung (Tsushima) Basin in the East (Japan) Sea.
- The partitioning fluxes of organic carbon vary with water depth under the influence of sedimentation rates and lateral transport.
- The slope acts as depocenter, and the lateral transport leads to high organic carbon content in the Ulleung (Tsushima) Basin.

This article has been accepted for publication and undergone full peer review but has not been through the copyediting, typesetting, pagination and proofreading process which may lead to differences between this version and the Version of Record. Please cite this article as doi: 10.1029/2019JG005138

Abstract

With the total sediment oxygen uptake rates measured using an in situ benthic chamber, vertical distributions of organic carbon and sedimentation rates estimated by excess ^{210}Pb across the slope to the basin sediment of the southwestern region of the Ulleung (Tsushima) Basin (UB), the partitioning of organic carbon fluxes in the sediment was estimated to understand the biogeochemical cycles of organic carbon in the high productivity marginal sea. The results of depth attenuation of total oxygen uptake (TOU) demonstrate that the organic carbon oxidation of the UB sediment was 2.5 times higher than that obtained from the empirical relationship of the global's depth attenuation of TOU. Similar to TOU, the high mass accumulation rates observed in the slope region were 9.5 times higher than the rate in the basin, indicating that the slope may act as the depocenter of organic carbon. The organic carbon budget with water depth gradient implies that a significant fraction of the organic carbon deposited into sediment is supplied by lateral transport down the slope. Definite increasing C/N ratio with water depth indicates the refractory organic carbon seems to be successively transported later from shelf to slope. The total burial flux in the sediment of southwestern UB was estimated to be 0.46±0.04 Tg C y^{-1}, which is similar to the megadepocenter of the Congo River fan. Our results imply that the UB sediment may be an important biogeochemical reaction place, not only for organic carbon but also materials linked to primary production.

Plain Language Summary

Phytoplankton in surface water produce particulate organic carbon (POC) with uptake of nutrients and carbon through photosynthesis. The POC settles into deep water and is deposited onto surface sediment. Because a large proportion of POC degrades during settling, the POC reaching the sediment layer is a small percentage of the overall production. Within the sediment, POC may be considered as two parts: degradable and nondegradable. The degradable POC is preferentially fueled and changed to nondegradable POC. Consequently, the nondegradable POC is enriched with time since deposition due to being buried into deeper sediments. Concentrations of degraded and buried POC are important to gaining an understanding of the history of carbon cycles because they are closely linked with the primary production of carbon dioxide in the atmosphere and its removal. The degradation and burial POC were assessed in the southwestern Ulleung (Tsushima) Basin (UB) of East (Japan) Sea. It was found that POC degradation was gradually decreased as water depth increasing and burial into sediment was highest at the slope suggesting that degradation and burial are controlled by water depth, sedimentation rate, lateral transport, and organic carbon qualities. The distribution of sediments in the UB may be closely coupled with transport, remineralization, and redistribution of POC in the interior of the basin.

Index terms

4804 Benthic process, 4805 Biogeochemical cycles, 4806 Carbon cycles, 4863 Sedimentation, 4894 Instruments, sensors and techniques

Keywords

East (Japan) Sea; benthic chamber; organic carbon oxidation; mass budget of organic carbon; lateral transport; burial flux

1 Introduction

Even though the continental margin covers less than 20% of the total surface area of the ocean, about one-half (20–50%) of the total primary production (PP) of the ocean occurs in the surface water above the continental shelf and slope (Liu et al., 2000; Walsh, 1991; Wollast, 1991). The large fraction of particulate organic matter, produced by pelagic primary producers and/or entered from the continent, is deposited onto the shallow continental shelf and slope sediments (de Haas et al., 2002). Because of the high primary production (PP) of surface water in marginal seas compared with the open ocean, the quantification of biogeochemical cycles of organic carbon (OC) in sediment is essential to build the global OC mass budget (Anderson et al., 1988, 1994; Archer & Devol, 1992; Canfield, 1993; DeMaster et al., 2002; Muller-Karger et al., 2005; Rowe et al., 1988, 1994; Thomson et al., 2000).

The fact is that the sediment of a marginal sea acts as a major sink or source of OC in the ocean, which is an important issue for the global carbon cycle (Jahnke & Jahnke, 2000; Jahnke et al., 1990;; Reimers et al., 1992; Rowe et al., 2008; Walsh et al., 1985). Complicated physical forces in a marginal sea (eddies, upwelling along the coastline, downslope current near the benthic layer) have been suggested as the control mechanisms of OC inventory and flux in the sediment layer, and thus those are important keys to the OC budget (de Haas et al., 2002; Hedges & Keil, 1995). Furthermore, the OC degradation and burial of the sediment layer are also controlled by transport pathways, sedimentation rate (SR), PP, OC qualities, oxygen exposure time, etc. (Burdige, 2007; Müller & Suess, 1979). Therefore, the sedimentary mass balance of OC is the sum of net flux integrated over the biogeochemical reactions; however, the robust OC budget is still not well known.

Regarding the OC mass budget, the OC oxidation rate, a removal term, is estimated using the oxygen uptake rate of sediment or production rate of total inorganic carbon with in situ or laboratory incubation (Glud et al., 2008). Because oxygen is the most favorable oxidizer for organic matter degradation, the total oxygen uptake (TOU) rate of sediment has been widely applied as a proxy for the organic carbon oxidation rate by multiplying the respiration quotation ratio (C/O_2: 106/138) by TOU (Canfield et al., 2005). Commonly, it has been used for enclosure incubation techniques in both in situ and ex situ experiments. Given that oxygen in incubation water is wholly consumed by biotic and/or abiotic reactions following OC oxidation, it will gradually decrease during incubation, and thus its initial decreasing rate is represented as the OC oxidation rate (de Beer et al., 2005). Several lines of research suggest that in situ incubation for TOU measurement would give a more reliable result than ex situ measurements because the unknown factors (temperature alteration and its effect on benthic respiration increasing during sample treatment) can induce uncertainty (Glud, 2008; Hammond et al., 2004; Tengberg et al., 2004). In particular, these artifacts are remarkable for deep-sea sediment (>1000 m) (Glud, 2008).

The East (Japan) Sea (EJS) is one of the marginal seas in the northwest Pacific. The Ulleung (Tsushima) Basin (UB), which is in the southern part of the EJS is well known as a high PP zone among basins in the EJS (Yoo & Park, 2009). Complicated oceanographic features, eddies, upwelling, branching out of surface warm water, and a polar front are observed in the southwestern part of the UB. These oceanographic events have been presented as the major driving forces to enhance PP in the euphotic depth (Hyun et al., 2009; Kim et al., 2012; Kwak et al., 2013a, b; Park et al., 2007; Yoo and Park, 2009) and may lead to a high export of OC to the deep sea (Kim et al., 2011). Although many studies have tried to understand the biogeochemical cycles of OC in the pelagic region, those in the benthic region are still limited (Hyun et al., 2010, 2017; Lee et al., 2008, 2010). In particular, the effects of the lateral transport of OC in sediment across the slope to the basin were not considered in

estimating the budget. Recently, the sediment trap data in the UB suggested that the particle fluxes from the water column were significantly higher than for other deep seas with no seasonality (Kwak et al., 2017), and the lateral transport of particulate materials near the bottom could significantly contribute to the vertical flux in the UB (Kim et al., 2017).

To understand the OC fate in the sediment of the UB, the OC mass budget across the slope to the basin must be estimated because the OC degradability with water depth can vary and the lateral transport of OC down the slope has been used as the major key to determine the sedimentary OC flux. Here, we first tried to estimate the OC budget across the shelf edge to the basin of the southwestern part of the UB. An autonomous in situ benthic chamber was developed to measure the robust TOU and benthic nutrient flux. With compiling of in situ TOU, SR, and the vertical distribution of OC contents in the sediment, a partitioning of OC fluxes was built to construct the OC mass budget across the water depth. We present and validate the sedimentary OC flux, and discuss the importance of margin sediment of the UB as the places for active biogeochemical reaction.

2 Materials and Methods

2.1 Study area

The EJS, located in the far eastern part of the Eurasian continental margin, is one of the deepest marginal seas (maximum depth: 3800 m, average depth: 1650 m) in the northwestern Pacific (Fig. 1). The surface area of the EJS covers approximately 1.01×10^6 km^2 (Lee et al., 2016) and is connected with four narrow shallow straits (Korea, Tsugaru, Soya, and Tartarsky). In the southern part of the EJS, the UB is one of the three major basins (UB, Japan Basin, and Yamato Basin), faced with the entrance of oligotrophic warm water (Tsushima current) that branches out and meanders along the coastline of Korea. The seasonal dynamical oceanographic features in the surface water of the UB are formation factors for eddies, coastal upwelling, and polar front emergence (Park et al., 2007, 2012). Kwak et al. (2013a) reported the monthly PP variations of the UB (annual mean = 273 g C m^{-2} y^{-1}) may be determined by water column stability and may be considerably higher than in the other regions of EJS (Russian coast and middle of Japan Basin). The high PP in surface water enhanced by the above physical forces (Kwak et al., 2013a, b; Yoo et al., 2009) may increase the OC content of the surface sediment (>4%) (Cha et al., 2005; Hyun et al., 2009).

The northern and eastern margins of the UB are characterized by the slope, which is relatively straight and steep (>10°), compared with those of the southern and western margins (1–2°) (Lee et al., 2016). The sedimentation rates across the slope to the basin ranged from 0.02 to 0.31 cm y^{-1}, being higher in the slope region and lower in the basin (Cha et al., 2005). Cha et al. (2005) suggested that the burial of phosphorus (P) in the sediment layer may be controlled by sedimentation rates, and digenetic redistribution of P occurs broadly in the continental margin and basin.

The dashed square box in Fig. 1 is an arbitrary boundary of the southwestern part of the UB (west, east, south, north = 129.64° E, 131.54° E, 35.45° N, 37.42° N). The total area of the box is approximately 3.7×10^4 km^2, which corresponds to about 3.7% of the total surface area of the EJS. Based on the degree of the slope across the shelf edge to the basin (Koo et al., 2004), the stations were classified into three groups: 1) 300–800 m water depth that has the steepest slope (>5.5°: shelf edge to upper-slope deposited by slump and slide deposits) (ES-1, 2); 2) 800–1500 m that has a moderate slope (2.0–3.1°: lower-slope to rise deposited by debris-flow deposit) (ES-3, 4, 5); and 3) >1500 m water depth which has the lowest slope (<0.8°) (ES-6, 7, 8, 9: rise to basin deposited by turbidites) (Table 1). The slump

and slide deposit, debris-flow deposit, and turbidites are zoned sequentially with a contour parallel of 300–800 m, 800–1500 m, and >1500 m water depth, respectively (Lee et al., 1996; Koo et al., 2004). A simple classification with bathymetry was used overall for sedimentary and seismic facies (Cha et al., 2005; Lee et al., 1996). By using a GIS program (Global Mapper ver. 20, Blue Marble Graphics), the area of each zonation was calculated (Table 1).

2.2 In situ experiment

The in situ experiments were performed three times during the spring and summer of 2014 and 2015 (Table 1). The experimental locations were determined after considering water depth (325 m to 2230 m) and surface water pathways. By using the CTD (SBE911Plus, Seabird Electronics Inc., Bellevue, WA, USA), the vertical profiles of temperature, salinity, and dissolved oxygen in the water column were determined before and after the benthic lander deployments.

The autonomous free fall of an in situ benthic lander for deep-sea (3000-m rate) studies was developed to measure TOU and nutrient fluxes via the sediment–water interface (Lee et al., 2015) (Fig. 2). Briefly, the benthic lander is composed of a chamber and microprofiler. The chamber system (Belc*II*) is constructed with a rectangular poly(vinyl chloride) benthic chamber (29×29 cm^2), which is used to isolate and incubate a predetermined sediment surface area in close contact with a known volume of seawater. On the lid, the stirring system consisting of four stirring bars is fixed into a central axis, which is linked with a magnetic clutch. The rotation speed of the stirring bars is ≈30 rpm, so the diffusivity boundary layer thickness is around 300–700 μm at this speed (Lee et al., 2015). An oxygen optode (Aanderra, 4831) is also mounted on the lid and constantly measures the oxygen at 10 s time intervals. The in situ incubated water samples in the benthic chamber are sequentially collected by an automatic syringe water sampler (11 50-mL plastic syringes) with a preset time interval (120 h). To calculate the benthic chamber volume, the first syringe can inject bromide (Br^-) or cesium (Cs^+) solutions into the benthic chamber after the lid is closed. The lander was deployed freely from a research vessel and the distance from the ship to the system continuously monitored using an acoustic pinger (Teledyne Benthos, 865-A) until touchdown. After waiting for more than 24 h, the benthic lander ascended by releasing a weight. Immediately after lander recovery, the incubated syringes for water-sample collecting were unloaded from the water sampler and filtered with a 0.2 μm membrane filter. The samples were stored in a deep freezer (–20 °C) until analysis in the laboratory.

2.3 Sediment collection

The undisturbed sediment core samples were collected using the box corer. To collect a subsample, plexiglass tubes (8 cm i.d., 40 cm length) were carefully inserted into the sediment in the box corer. Both ends were capped with rubber stoppers. The cores were immediately transferred to a refrigerator to store until core sectioning. Within a few hours of sample collection, the sediment core was sectioned at 1 cm intervals to measure OC content and ^{210}Pb activity. The sediments were stored in a deep freezer (<–20 °C) until analysis.

2.4 Onboard incubation for sediment oxygen uptake ($TOU_{ex\ situ}$)

Using the incubation chamber for an onboard experiment, the undisturbed sediment samples were collected separately to measure the sediment oxygen uptake in the laboratory ($TOU_{ex\ situ}$) (Lee et al., 2015). Before anything else, the incubation chamber core was carefully inserted into the sediment with the bottom open and retrieved carefully. Both ends

were immediately closed with a gas-tight lid, leaving an internal water height of ≈6 cm, and then stored in a refrigerator to maintain the in situ temperature for a short time (<2 h). Before the experiment, the water temperature in the incubation water bath (EYELA, NTT-2100 and ECS-0) was controlled at the in situ temperature. The incubation chamber was submerged in a water bath. Using mass flow controllers (MFC Tech, AIR-500), the water in the incubation chamber was maintained at the in situ oxygen concentration by circulation using a pump. The oxygen concentration in the chamber was measured at 10 s intervals with an inline oxygen optode (Pyroscience, OXFTC2). With two-point calibration (zero concentration and air saturation of in situ bottom water), the optode sensors were calibrated at each station.

2.5 Laboratory analysis

The in situ incubated chamber water samples for nutrients (ammonium, nitrate, phosphate, and silicate) were measured using standard colorimetry methods (Hansen & Koroleff, 1999) on a flow injection autoanalyzer (Bran+Luebbe, QuAAtro39 AutoAnalyzer).

The sectioned sediment samples were treated to determine the water content using the weight loss after drying to constant weight at 105 °C. The dry bulk density (DBD, g cm^{-3}) was calculated from water contents and grain density, which was measured for dried samples using a He pycnometer (AccPyc 1340, Micromeritics Instrument Crop., USA). Using a CHN analyzer (Thermo Finnigan, Flash EA 1112), the total organic carbon (TOC) and nitrogen content of the sediments were measured after acidification with 1 M HCl.

The determination of excess ^{210}Pb ($^{210}Pb_{xs}$) in sediments is described in Lee et al. (2012). Assuming that the total activity of ^{210}Po (daughter nuclide of ^{210}Pb) in the sediments has reached radioactivity equilibrium with ^{210}Pb, the total ^{210}Pb activity was determined by measuring ^{210}Po. Briefly, the powdered sediment (≈0.5 to 1 g) was spiked with ^{209}Po tracer and then leached out with hot strong acid. To reduce the ferric ions, ascorbic acid was added to the acidified filtrate solution, and then the Po isotopes (^{209}Po and ^{210}Po) were spontaneously deposited onto a silver disk at 70 °C over a period of 6 h with stirring. The measurement of activity was continued to obtain sufficient counts (>1000) by an alpha particle spectrometer equipped with low-background silicon-surface barrier detectors (PIPS detector, Canberra, USA) (Lee et al., 2012). The $^{210}Pb_{xs}$ was calculated by subtracting the value for supported ^{210}Pb, the average of ^{210}Pb activities in the deep sediment layer.

2.6 Calculation

The TOU and benthic nutrient flux were estimated from a least squares linear regression using the concentration gradients with time and depth of the benthic chamber as follows:

$$F = \left(\frac{dC}{dt}\right) \times \frac{V}{A}, \quad (1)$$

where F is the TOU and benthic nutrient fluxes (mmol m^{-2} d^{-1}), dC/dt is the gradient of the linear regression line estimated from fitting the concentration "C" as a function of the incubation time "t" (mmol dm^{-3} d^{-1}), V is the chamber volume (m^3), and A is the chamber area (m^2).

The SR was estimated from the slope of $^{210}Pb_{xs}$ activity with sediment depth. Assuming a steady state ($dC/dt = 0$), the activity of $^{210}Pb_{xs}$ (R) at a specified depth is dependent on the activity at time 0 (R_0), ^{210}Pb (λ) decay constant, and time. The SR is a function of time (y) and depth (cm), i.e., SR = z/t, and these relationships can be formulated as follows:

$$R = R_0 \exp\left(-\frac{\lambda}{SR} z\right), (2)$$

where R is the $^{210}Pb_{xs}$ activity at each specific depth of sediment, R_0 is the $^{210}Pb_{xs}$ activity in the surface sediment, λ is the ^{210}Pb decay constant (0.031 y^{-1}), and SR is the sedimentation rate (cm y^{-1}). SR is derived from the slope of the regression line of data estimated using the linearized version of Eq. (2).

The sediment mass accumulation rate (MAR) and organic carbon burial fluxes (OC_{burial}) at the lowest sediment layer were calculated with the following equations:

$$MAR = DBD \times SR, (3)$$

$$OC_{burial} = MAR \times OC_{\infty}, (4)$$

where MAR is the mass accumulation rate (g m^{-2} y^{-1}), DBD is the mean dry bulk density (g cm^{-3}) that shows the constant values of the lowest three layers of sediment, SR is the sedimentation rate below the mixed layer (cm y^{-1}), OC_{burial} is the burial fluxes of organic carbon (g m^{-2} y^{-1}), and OC_{∞} is the mean organic carbon content (%) at the lowest three layers of sediment.

Assuming a steady state, the OC mass budget was calculated as the following equation (Martens & Klump, 1984):

$$OC_{in} = OC_{ox} + OC_{burial}, (5)$$

where OC_{in} is the input flux of OC into sediment from the water column, OC_{ox} is the flux of the oxidation of organic carbon that is determined by multiplying TOU and the Redfield ratio (106/138), and OC_{burial} is the burial flux of organic carbon.

3 Results

The experimental times, locations, water depths, salinities, temperatures, and oxygen concentrations (O_2) of bottom water at each station are listed in Table 1. The bottom water temperatures ranged from 0.16 to 0.71 °C, which was highest at ES-1, but the salinities of bottom water were spatially uniform. The O_2 of bottom water ranged from 173 to 217 μmol dm^{-3}, which was similar to other marginal seas (e.g., Mid-Atlantic continental slope: Jahnke and Jahnke, 2000; Iberian margin: Epping et al., 2002; Gulf of Mexico: Rowe et al., 2008; Southeast Atlantic margin: Rabouille et al., 2009).

3.1 Total oxygen uptake rate

The evolution of O_2 in the benthic chamber with increasing time is shown in Fig. 3. With increasing time, the O_2 concentration gradually decreased because of the benthic mineralization of organic matter in the sediment. Using the slope of the linear relationship between increasing time and decreasing oxygen (dO_2/dt), the TOUs following the water depth gradient were estimated. However, the in situ measurements of TOU at ES-1 and ES-6 failed because of data logger problems of Belc*II*; thus, those were replaced with the onboard incubation ($TOU_{ex\ situ}$) result (Table 2). The TOU range was between 2.0 and 12.1 mmol O_2 m^{-2} d^{-1}, which was highest at ES-1 and lowest at ES-9 (Table 2). At ES-6, the result of onboard incubation significantly departed from the overall trend. The relationship between TOU and water depth showed a good exponentially decreasing function (TOU = 20.89 exp (–0.002227)z + 2.084, R^2 = 0.98), except for ES-6, and the asymptotic value of the function was found to be 2.084 mmol m^{-2} d^{-1}. This value agreed well with the previous results of sediment oxygen uptake rate of the UB sediment (Lee et al., 2010). At the same locations of ES-3 (950 m) and ES-5 (1450 m) in Oct and Nov 2013, two Belc*II* were deployed to test the

Belc*II* system (Lee et al., 2015). The in situ TOU were 5.80 and 3.77 mmol O_2 m^{-2} d^{-1} at ES-3 and ES-5, respectively, which agreed well with our results.

3.2 Benthic nutrient flux

The evolutions of nutrients (ammonium, sum of nitrate, phosphate, and silicate) with increasing time are represented in Fig. 4. Overall, they gradually increased with increasing time due to organic matter degradation in the surface sediment. From the linear relationship of nutrient concentrations with increasing time, the benthic nutrient fluxes were also calculated and are listed in Table 2. Interestingly, the sum of nitrate and nitrite (hereafter called nitrate flux) in the slope sediment were significantly decreased, which was expected from the denitrification or anammox processes. The ammonium, nitrate, phosphate, and silicate benthic fluxes were estimated and were found to range from –0.016±0.007 to 0.21±0.02, –0.43±0.08 to 1.7±0.3, 0.006±0.003 to 0.15±0.02, and 2.0±0.1 to 7.5±1.8 mmol m^{-2} d^{-1}, respectively. Those are comparable with previous results (Lee et al., 2015).

3.3 Vertical distribution of OC_{org}

Overall, the OC_{org} contents decreased vertically with increasing sediment depth except for ES-1. The OC_{org} contents of ES-1 were significantly lower than for other stations. The "dilution effect" by coarse grain size sediment may explain the low OC content at ES-1 (Khim et al., 1997). The OC_{org} of the surface (OC_0: 0–1 cm) and mean lowest sediment (OC_∞) ranged from 1.80 to 2.95% and from 1.56 to 2.15%, respectively (Table 3). At water depth of < 1000 m, the surface OC_0 gradually increased with increasing water depth, and then were constant within a narrow range (2.55–2.95%). By contrast, the OC_∞ at <1000 m water depth stations increased as the OC_0 increased and both decreased with increased water depth. In particular, the differences between C_0 and C_∞ also increased with water depth, which showed a positive linear relationship with water depth ($(C_0 - C_\infty)$ = 0.0005 water depth – 0.0143, R^2 = 0.82) (Fig. 6).

3.4 Mass accumulation rate (MAR) and OC burial flux

At ES-1, ES-2, ES-6, ES-7, and ES-8, the surface mixed layers reached approximately 10 cm (Fig. 7). The apparent sedimentation rates (ASRs) including the biological mixing effect of the surface mixed layer ranged from 0.06 to 0.86 cm y^{-1}. The SRs under a mixed layer of sediment across the slope to the basin ranged from 0.06 to 0.49 cm y^{-1}, which generally decreased with increased water depth (Table 3). In particular, the SRs of the slope sediment (ES-1 to ES-4; <1285 m water depth) were higher than the same at deeper sites. Our SR results agree with those of previous studies (Cha et al., 2005; Hong et al., 1997; Kim & Park, 2003; Lee et al., 2010).

MARs, products of mean DBD of the lowest core and SR (Eq. 3), ranged from 228 g m^{-2} y^{-1} to 2016 g m^{-2} y^{-1} (mean: 991±809 g m^{-2} y^{-1}) and showed a large spatial difference (Table 3). In the slope (ES-2, ES-3, and ES-4), the MAR was 9.5 times higher than the MAR in the basin. Hong et al. (1997) also suggested that the MARs in the slope of the southwestern part of UB were up to three times larger than those in other basins of EJS.

Burial fluxes of OC ranged from 3.0±0.1 to 48.6±4.3 g C m^{-2} y^{-1} (mean: 20.8±2.7 g C m^{-2} y^{-1}) (Table 4), which are comparable with other marginal sea sediment fluxes (Table 5). The distribution of those values with water depth shows that a significantly higher OC_{burial} (>40 g C m^{-2} y^{-1}) is shown at water depths shallower than 1285 m (ES-2 to ES-4) and then rapidly decreases below that water depth.

4 Discussion

Sedimentary OC mass balance represents the net partitioning fluxes, i.e., 1) the vertically and/or laterally transported OC fluxes from the water column equals the sum of 2) remineralization fluxes and 3) burial fluxes into the deep sedimentary layer assuming the steady state (Burdige, 2007). Each flux can be spatiotemporally varied and controlled with various oceanographic/biogeochemical factors (Burdige, 2007; Emerson & Hedges, 1988; Hedges & Keil, 1995). For example, the vertical flux of particulate OC is enhanced by the high PP in the euphotic zone, and thus it leads to high accumulation of OC in the surface sediment (Jahnke, 1996; Müller & Suess, 1979). In the continental margin, half of the input OC to the sea floor is deposited within 500 km of the continental slope by near-bottom lateral transport or biological transport (Jahnke et al., 1990). UB Basin has a relatively small horizontal scale across the slope to the basin compared with other marginal seas and it is walled off from the slope of the basin. These topographic characteristics may allow the OC in deep water to be scraped to the basin sediment by downslope transport. Therefore, the lateral transport of OC down the slope, a typical characteristic of the continental margin, needs to be evaluated with the partitioning of OC across the slope to the basin to understand the fate of OC in UB.

4.1 Depth attenuation of TOU

As mentioned above, the in situ TOU measurement at ES-1 and ES-6 failed due to an electronics problem with the data logger. To discuss the depth attenuation of TOU, the onboard incubation results at ES-1 and ES-6 were tested to substitute for the in situ results. However, the TOU rate at ES-6 significantly departed from the overall trend with water depth relationship (Table 2).

Our empirical relationship of depth attenuation of in situ TOU yielded $\mathrm{TOU} = 2617WD^{-0.925}$ ($R^2 = 0.86$). By substituting the depth of ES-1 (365 m) to the relationship, the TOU was given as 12.4 mmol m^{-2} d^{-1}, which agrees well with the onboard incubation results. By contrast, the calculated TOU at ES-6 was 2.7 mmol m^{-2} d^{-1}, corresponding to 34% of the onboard incubation results. This contrary result with water depth can be explained by the requirement time for the sample pretreatment. Because of the shallow water depth in ES-1, the retrieve time of the box core was about five times less than ES-6, possibly minimizing the temperature alteration effect on the sediment sample. It is well known that a discrepancy in deep water sediment (>1000 m) between in situ and onboard incubation could arise during sample treatment (alteration of temperature and stress, underrepresentation of benthic fauna) and affect TOU measurement (Glud, 2008; Glud et al., 1999; Hammond et al., 2004; Sauter et al., 2001; Wenzhöfer & Glud, 2002;). Indeed, the onboard TOUs of the UB at water depths more than 1000 m were 2.0 to 2.3 times higher than the in situ results, and suggest that the temperature alteration during sample treatment could alter the TOU results because the bottom water temperature of the UB is less than 0.3 °C (Lee et al., 2015). Therefore, we exclude the TOU of ES-6 in further discussion.

Depth attenuation of TOU represents the integrated effects on OC degradation until burying into the deep sediment layer, which is controlled by PP, OC degradability with quality, sinking speed of particulate OC in the water column, etc. (Andersson et al., 2004). Within about two orders of magnitude, the global depth attenuation of TOU varies with water depth from 100 m to 2000 m (Fig. 8) (Glud, 2008). Our TOU are assessed as 2.1–3.2 (mean: 2.5) times higher than the modeled results calculated based on the global empirical relationship (TOU = 284 water $\mathrm{depth}^{-0.74}$) (Glud, 2008). This result may imply that 1) OC contents in the sediment of the UB are higher than in other open oceans, 2) deposited OC of

the UB sediment may contain labile OC, and 3) oxygenated bottom water of the UB may enhance the benthic respiration despite the low temperature of the bottom water.

Given that TOU is represented as the sum of oxidant consumption for OC degradation processes in the sediment layer, it can be converted to organic carbon oxidation rate (OC_{ox}) by applying the Redfield ratio (O_2:C, 138/106). The OC_{ox} ranged from 1.5 to 9.3 mmol C m^{-2} d^{-1} (6.6–40.8 g C m^{-2} y^{-1}), which corresponded to 2.4–14.9% of primary production (PP = 273 g C m^{-2} y^{-1}, Kwak et al., 2013a; Kim et al., 2017) in the UB.

4.2 Burial flux of OC in the UB sediment

The burial OC fluxes accounted for 1.3% to 17.8% of the annual mean PP of the UB, which also stands out in the region <1285 m. Lee et al. (2010) reported that the average OC_{burial} flux below 2000 m at the center of the UB was 2.59 g C m^{-2} y^{-1}, which corresponds to 70% of our result. Burial flux of OC shows a strong positive linear relationship with SR (OC_{burial} = 92.22SR + 0.97, R^2 = 0.95), implying that the SR may act as the main control factor on OC preservation (Fig. 9) (Hedges & Keil, 1995; Müller & Suess, 1979). Similar to the zonations based on the slope from the shelf edge to basin, the OC_{burial} flux and SR at each station were also categorized into three groups, i.e., 1) the high SR and OC_{burial} at ES-2 to ES-4, 2) the low SR and OC burial at ES-6 to ES-9, and 3) the shelf edge (ES-1) and the station between the lower-slope and the rise (ES-5).

4.3 Mass budget of OC across the slope to the basin

In Table 4, the partitioned OC flux in the sedimentary layer (OC_{ox}, OC_{burial}, and OC_{in} = OC_{ox} + OC_{burial}), the vertical flux of OC (J_{in}) from the water column calculated using an empirical relationship between water depth and PP (Berger et al., 1987), burial efficiency (BE) ((OC_{burial}/OC_{in}) × 100), and the ratio OC_{in}/J_{in} are listed. Consistently, the stations across the shelf edge to the basin were categorized into three groups based on their degree of geomorphology, MAR, $OC_{burial\ flux}$, and BE: 1) the shelf edge to the upper slope (ES-1 and ES-2), 2) the lower slope to the rise (ES-3 to ES-5), and 3) the rise to the basin (ES-6 to ES-9). Each partitioning of OC fluxes across the shelf edge to the basin is represented in Fig. 10. Spatially, the fluxes with water depth are distinguished; i.e., OC_{in} and OC_{burial} at < 1500 m were higher by a factor of greater than 4 and 6 times more than the basin, respectively.

Given that J_{in} can be represented for the vertical fluxes following PP in the euphotic depth of surface water and the C_{in} may be the sum of lateral and vertical fluxes of OC, the difference between OC_{in} and J_{in} (OC_{lat} = OC_{in} – J_{in}) can be represented as the lateral flux (OC_{lat}) of OC, which may be transported by the downslope current. The OC_{lat} were found to average 48.8 ± 3.5 g C m^{-2} y^{-1} from the shelf edge to upper-slope, 39.4 ± 2.5 g C m^{-2} y^{-1} from the lower-slope to basin, and 6.7 ± 0.3 g C m^{-2} y^{-1} from the rise to basin, which also decreased with increasing water depth (Table 4). By contrast, the BEs and the ratios OC_{in}/J_{in} at ES-3 and ES-4, located in the lower-slope, are higher than at other stations, suggesting that the lateral transport of OC down the slope was focused in the upper- to lower-slope region. The sediment failure scare was observed with our experiment in the range from 300 m to 800 m water depth, and it caused the mass transport deposit to lower-slope sediment (Koo et al., 2014). The seismic data also suggest that the debris-flow deposits had a stratified thickness more than 1 m at the sediment cores around a water depth of 800–1200 m. These results are well matched with our results, which have significantly higher MAR and BE around a water depth of 680–1300 m, suggesting that the region between the upper-slope and the lower-slope may be a “depocenter of OC” in the southwestern part of the UB. In several studies of marginal seas, an “OC depocenter” has been observed with higher SR, OC content of

sediment, and BE (Anderson et al., 1994; Rabouille et al., 2009), encompassing the mid-slope region.

4.4 Evidence of lateral transport of OC across the shelf to the basin

The lateral transport of OC across the shelf to the basin in the continental margin has been studied to estimate the OC budget because the downslope transport of OC can significantly contribute to the total OC budget in the sediment (Alperin et al., 2002; Anderson et al., 1994; Jahnke & Jahnke, 2000; Rabouille et al., 2009). In general, the natural radioisotope ^{210}Pb (half-life of 22.3 years) has been used as a tracer to estimate the cross-slope transfer of particles in marginal seas (Bacon et al., 1994; Biscaye & Anderson, 1994; Lepore et al., 2009; Schmidt et al., 2009; van Weering et al., 2002) because its geochemical property is particle reactive and its production and decay in the sediment is possible to predict with ^{226}Ra activity and the decay constant of ^{210}Pb. The lack of balance of the $^{210}Pb_{xs}$ budget ($^{210}Pb_{xs}$ support from atmosphere and water column $\neq$ sedimentary $^{210}Pb_{xs}$ flux) in the sediment implies that the particles could be laterally added or swept off by the downslope current across the slope to the basin. Indeed, the sedimentary $^{210}Pb_{xs}$ fluxes in the southwestern part of the slope in the UB were 1.3 to 2.1 times higher than the sum of atmospheric flux and production flux in the water column, which indicates the lateral exporting of particles from the shelf to the basin (Kim and Park, 2003).

The vertical particulate organic carbon (POC) fluxes from May to August 2011 collected in the sediment trap at depth (<2000 m) of the UB ranged from 2.9 to 20.8 (average: 9.8 ± 2.1 g C m^{-2} y^{-1}, n = 9) (Kim et al., 2017). Interestingly, the vertical POC fluxes at 1000 m and 2300 m depth collected at the nearby ES-9 were estimated to be 9.0 and 9.8 g C m^{-2} y^{-1}, respectively, somewhat higher at a deeper depth. Considering the depth attenuation of POC flux (Suess, 1980), the higher flux at deeper depth implied that the additional POC (resuspension and allochthonous POC) would contribute to the vertical POC flux. Likewise, J_{in} at 1000 m was found to be 7.9 g C m^{-2} y^{-1}, corresponding to 87% of the POC flux collected by the sediment trap, but J_{in} at 2300 m was 49% of the POC flux, which could be explained by the lateral transport effect. Furthermore, the allochthonous POC collected in the sediment trap at 2300 m accounted for approximately 30% to 50% of the total flux with the signature of Δ^{14}C values and Al mass balance even though ES-9 is far away from the continental shelf (Kim et al., 2017).

Hyun et al. (2017) observed that a thick manganese oxide layer is covered by the surface sediment layer of the slope and basin sediment of the UB. They calculated that the manganese oxide of surface sediment is reoxidized 3600 times before permanent burial. The pathway of manganese oxide in the sediment layer seems to be coupled with biological mixing (bioirrigation and bioturbation) and lateral transport down the slope. Long spatial pathways across the slope to the basin can enhance the Mn oxidation (Mn^{2+} to MnO_4^-) and progressively carry it to the basin of the UB. The relationship between C/N molar ratio and depth also supports the progressive lateral transport of OC down the slope (Fig. 11). The degradability of OC can change from labile to refractory far away from its source, i.e., the C/N ratio can increase following deeper and farther along the slope, if the spatial distance (water depth and distance from the shelf) can represent the travel time of the OC. Given that the labile OC is oxidized preferentially with the downslope transfer, the refractory OC fraction in the sediment can be enriched. This segregation following OC degradability can explain why TOU varies with water depth but not OC content of the sediment. To confirm our explanations, further study is required using tracers (biomarkers, stable isotopes) for measuring OC qualities (Burdige, 2007).

4.5 Comparison with other marginal sediments

Across the slope to the basin in a marginal sea, the OC fate and behavior are important because they are related to the sink for carbon dioxide in the atmosphere and/or energy source for deep-sea ecosystems (Anderson et al., 1988; Epping et al., 2002; Jahnke et al., 1990; Rowe et al., 1998; Smith, 1983; van Weering et al., 2002). The results presented here show that the OC oxidation of the UB sediment is at a higher compared with other deep-sea sediments (Lee et al., 2008), and the BEs in the slope sediment are also remarkably higher than for most margin sediments (Table 5). With outstanding SR and OC burial fluxes on upper- to lower-slope regions, the OC depocenter exhibits similar water depth to other marginal slope sediments (Mid-Atlantic Bight, Iberian Margin) (Anderson et al., 1994; Biscaye & Anderson, 1994; Epping et al., 2002).

The total area of the southwestern part of the UB is approximately 3.7×10^4 km^2, which corresponds to about 3.7% of the total surface area of the EJS. The calculated areas from the shelf edge to the upper-slope (300–800 m), from the lower-slope to the rise (800–1500 m), and from the rise to the basin (> 1500 m) are 0.4×10^4 (11% of the total area), 0.7×10^4 (18% of the total area), and 2.1×10^4 km^2 (55% of the total area), respectively. Burial of OC in each region was found to be 0.12±0.04 Tg C y^{-1} from the shelf edge to the upper-slope, 0.24±0.02 Tg C y^{-1} from the lower-slope to the rise, and 0.11±0.01 Tg C y^{-1} from the rise to the basin; about 78% of total OC flux is buried in the shelf edge to the slope, even though it covered only 29% of the total area. The OC burial in the sediment of the East China Sea (ECS) shelf, one of the marginal seas in the west Pacific, was found to be 7.4 Tg C y^{-1}, which is assessed as a sink for both terrestrial and marine OC (Deng et al., 2006). Apparently, the total area of the southwestern part of the UB and OC burial in this area correspond to 4.2 and 6.2% of the ECS, respectively. Although our estimation corresponds to a few percent compared with the ECS shelf and it contributes a small portion to the global amount, the burial OC capacities into the sediment of UB may provide intriguing information because there are no large rivers directly connected to the UB and it is deeper than the ECS shelf. Furthermore, the total burial OC must be underestimated because our estimation is represented as just the southwestern part of UB. Lastly, our results correspond to the value of the megaburial center in the Congo submarine fan (0.4 Tg y^{-1}), which is the pathway of terrestrial OM from the Congo River in Africa.

5 Summary

Based on the partitioning of OC fluxes across the slope to the basin of the UB, estimated using in situ TOU, MAR, and OC_{org} contents of the sediment, the following highlights were found. The depth attenuation of TOU of the UB suggested that the OC oxidation is 2.5 times higher than the other deep-sea sediments and may be partitioned followed by vertical and/or lateral transport down the slope. In the slope, the significantly higher MAR would control the OC burial flux with high burial efficiency, which acts as an OC depocenter and energy source for the deep-sea ecosystem of the UB. The downslope transport of the OC flux onto sediment was significantly higher at the slope region and its reworking processes can cover the whole UB because of its small horizontal scale. The refractory fraction of OC is spatially segregated, which is a major control key on biogeochemical cycles of materials.

Acknowledgments

This work was fully supported by the Korea Institute of Ocean Science and Technology (PE99613 and PE99711) and the Ministry of Oceans and Fisheries (PG51010, 20180040: Deep Water Circulation and Material Cycling in the East Sea). We thank the crews of the *R/V EARDO* for benthic lander operation and sampling assistance. In addition, the authors thank the two anonymous reviewers for their helpful comments that improved the early version of the manuscript. The authors declare that the research was conducted in the absence of any commercial or financial relationships that could be a potential conflict of interest. The research data can be accessed at the following repository: https://github.com/leejs728/eastsea_org.

References

Alperin, M.J., Suayah, I.B., Benninger, L.K., & Martens, C.S. (2002). Modern organic carbon burial fluxes, recent sedimentation rates, and particle mixing rates from the upper continental slope near Cape Hatteras, North Carolina (USA). *Deep-Sea Research II* 49, 4645–4665. https://doi.org/10.1016/S0967-0645(02)00133-9

Anderson, R.F., Bopp, R.F., Buesseler, K.O., & Biscaye, P.E. (1988). Mixing of particles and organic constituents in sediments from the continental shelf and slope off Cape Cod: SEEP-I results. *Continental Shelf Research* 8, 925–946. https://doi.org/10.1016/0278-4343(88)90082-9

Anderson, R.F., Rowe, G.T., Kemp, P.F., Trumbores, S., & Biscaye, P.E. (1994). Carbon budget for the mid-slope depocenter of the Middle Atlantic Bight. *Deep-Sea Research II* 41, 669–703. https://doi.org/10.1016/0967-0645(94)90040-X

Andersson, J.H., Wijsman, J.W.M., Herman, P.M.J., Middelburg, J.J., Soetaert, K., & Heip, C. (2004). Respiration patterns in the deep ocean. *Geophysical Research Letters* 31, L03304. https://doi.org/10.1029/2003GL019754

Archer, D.E., & Devol, A.H. (1992). Benthic oxygen fluxes on the Washington shelf and slope: a comparison of in situ microelectrode and chamber flux measurements. *Limnology and Oceanography* 37, 614–629. https://doi.org/10.4319/lo.1992.37.3.0614

Bacon, M.P., Belastock, R.A., & Bothner, M.H. (1994). ^{210}Pb balance and implications for particle transport on the continental shelf, U.S. Middle Atlantic Bight. *Deep-Sea Research II* 41, 511–535. https://doi.org/10.1016/0967-0645(94)90033-7

Berelson, W.M., McManus, J., Coale, K.H., Johnson, K.S., Kilgore, T., Burdige, D., & Pilskaln, C. (1996). Biogenic matter diagenesis on the sea floor: A comparison between two continental margin transects. *Journal of Marine Research* 54, 731–762. https://doi.org/10.1357/0022240963213673

Berger, W.H., Fischer, K., Lai, C., & Wu, G. (1987). Ocean productivity and organic carbon flux. I. Overview and maps of primary production and export production. University of California, San Diego, SIO Reference, 87-30, 67 pp.

Betts, J.N., & Holland, H.D. (1991). The oxygen content of ocean bottom waters, the burial efficiency of organic carbon, and the regulation of atmospheric oxygen. *Palaeogeography Palaeoclimatology* 97, 5–18. https://doi.org/10.1016/0031-0182(91)90178-T

Bhushan, R., Dutta, K., & Somayajulu, B.L.K. (2001). Concentrations and burial fluxes of organic and inorganic carbon on the eastern margins of the Arabian Sea. *Marine Geology* 178, 95–113. https://doi.org10.1016/S0025-3227(01)00179-7

Biscaye, P.E., & Anderson, R.F. (1994). Fluxes of particulate matter on the slope of the southern Middle Atlantic Bight: SEEP-II. *Deep-Sea Research II* 41, 459–509. https://doi.org/10.1016/0967-0645(94)90032-9

Burdige, D.J. (2007). Preservation of organic matter in marine sediments: controls, mechanisms, and an imbalance in sediment organic carbon budgets? *Chemical Reviews* 107, 467–485. https://doi.org/10.1021/cr050347q

Canfield, D.E. (1993). Organic matter oxidation in marine sediments. In R. Wollast, L. Chou, F. Mackenzie (Eds.), Interactions of C, N, P and S Biogeochemical Cycles and Global Change (pp. 333–356). Springer, New York, NY. https://doi.org/10.1007/978-3-642-76064-8

Canfield, D.E., Kristensen, E., & Thamdrup, B. (2005). Aquatic Geomicrobiology. Elsevier, New York, pp. 640.

Cha, H.J., Lee, C.B., Kim, B.S., Cho, M.S., & Ruttenberg, K.C. (2005). Early diagenetic redistribution and burial of phosphorus in the sediments of the southwestern East Sea (Japan Sea). *Marine Geology* 216, 127–143. https://doi.org/10.1016/j.margeo.2005.02.001

de Beer, D., Wenzhöfer, F., Ferdelman, T.G., Boehme, S.E., Huettel, M., van Beusekom, J.E.E., Böttcher, M.E., Musat, N., & Dubilier, N. (2005). Transport and mineralization rates in North Sea sand intertidal sediment, Sylt–Rømø Basin, Wadden Sea. *Limnology and Oceanography* 50, 113–127. https://doi.org/10.4319/lo.2005.50.1.0113

de Haas, H., van Weering, T.C.E., & de Stigter, H. (2002). Organic carbon in shelf seas: sinks or sources, processes and products. *Continental Shelf Research* 22, 691–717. https://doi.org/10.1016/S0278-4343(01)00093-0

DeMaster, D.J., Thomas, C.J., Blair, N.E., Fornes, W.L., Plaia, G., & Levin, L.A. (2002). Deposition of bomb ^{14}C in continental slope sediments of the Mid-Atlantic Bight: assessing organic matter sources and burial rate. *Deep-Sea Research II* 49, 4667–4685. https://doi.org/10.1016/S0967-0645(02)00134-0

Deng, B., Zhang, J., & Wu, Y. (2006). Recent sediment accumulation and carbon burial in the East China Sea. *Global Biogeochemical Cycles* 20, GB3014, https://doi.org/10.1029/2005GB002559.

Emerson, S., & Hedges, J.I. (1988). Processes controlling the organic carbon content of open ocean sediments. *Paleoceanography paleoclimatology* 3, 621–634. https://doi.org/10.1029/PA003i005p00621

Epping, E., van der Zee, C., Soetaert, K., & Helder, W. (2002). On the oxidation and burial of organic carbon in sediments of the Iberian margin and Nazaré Canyon (NE Atlantic). *Progress Oceanography* 52, 399–431. https://doi.org/10.1016/S0079-6611(02)00017-4

Glud, R.N., 2008. Oxygen dynamics of marine sediment. *Marine Biology Research* 4, 243–289. https://doi.org/10.1080/17451000801888726

Glud, R.N., Gundersen, J.K., & Holby, O. (1999). Benthic in situ respiration in the upwelling area off central Chile. *Marine Ecology Progress Series* 186, 9–18. https://www.jstor.org/stable/24853288

Hammond, D.E., Cummins, K.M., McManus, J., Berelson, W.M., Smith, G., & Spagnoli, F. (2004). Methods for measuring benthic nutrient flux on the California Margin: Comparing shipboard core incubations to in situ lander results. *Limnology and Oceanography: Methods* 2, 146–159. https://doi.org/10.4319/lom.2004.2.146

Hansen, P.H., & Koroleff, F. (1999). Determination of nutrients. In K. Grasshoff, K. Kremling, M. Ehrhardt (Eds.), Methods of Seawater Analysis (pp. 159–228). Wiley–VCH, Germany. https://doi.org/10.1002/9783527613984

Hartnett, H.E., & Devol, A.H. (2003). Role of a strong oxygen-deficient zone in the preservation and degradation of organic matters: A carbon budget for the continental margins of northwest Mexico and Washington State. *Geochimica Cosmochimica Acta* 67, 247–264. https://doi.org/10.1016/S0016-7037(02)01076-1

Hedges, J.I., & Keil, R.G. (1995). Sedimentary organic matter preservation: an assessment and speculative synthesis. *Marine Chemistry* 49, 81–115. https://doi.org/10.1016/0304-4203(95)00008-F

Henrichs, S.M., & Farrington, J.W. (1984). Peru upwelling region sediment near 15°S. 1. Remineralization and accumulation of organic matter. *Limnology and Oceanography* 29, 1–19. https://doi.org/10.4319/lo.1984.29.1.0001

Hong, G.H., Kim, S.H., Chung, C.S., Kang, D.-J., Shin, D.-S., Lee, H.J., & Han, S.-J. (1997). ^{210}Pb-derived sediment accumulation rates in the southwestern East Sea (Sea of Japan). *Geo-Marine Letters* 17, 126–132. https://doi.org/10.1007/s003670050017

Hyun, J.-H., Kim, D., Shin, C.-W., Noh, J.-H., Yang, E.-J., Mok, J.-S., Kim, S.-H., Kim, H.-C., & Yoo, S. (2009). Enhanced phytoplankton and bacterioplankton production coupled to coastal upwelling and an anticyclonic eddy in the Ulleung basin, East Sea. *Aquatic Microbial Ecology* 54, 45–54. https://doi.org/10.3354/ame01280

Hyun, J.-H., Kim, S.-H., Mok, J.-S., Cho, H., Lee, T., Vandieken, V., & Thamdrup, B. (2017). Manganese and iron reduction dominate organic carbon oxidation in deep continental margin sediments of the Ulleung Basin, East Sea. *Biogeosciences* 14, 941–958. https://doi.org/10.5194/bg-14-941-2017

Hyun, J.-H., Mok, J.-S., You, O.-R., Kim, D., & Choi, D.-L. (2010). Variations and controls of sulfate reduction in the continental slope and rise of the Ulleung Basin off the southeast Korean upwelling system in the East Sea. *Geomicrobiology Journal* 27, 212–222. https://doi.org/10.1080/01490450903456731

Jahnke, R.A. (1996). The global ocean flux of particulate organic carbon: Areal distribution and magnitude. *Global Biogeochemical Cycles* 10, 71–88. https://doi.org/10.1029/95GB03525

Jahnke, R.A., & Jahnke, D.B. (2000). Rates of C, N, P and Si recycling and denitrification at the US Mid-Atlantic continental slope depocenter. *Deep-Sea Research I* 47, 1405–1428. https://doi.org/10.1016/S0967-0637(99)00118-1

Jahnke, R.A., Reimers, C.E., & Craven, D.B. (1990). Intensification of recycling of organic matter at the sea floor near ocean margins. *Nature* 348, 50–54. https://doi.org/10.1038/348050a0

Khim, B.-K., Shin, D.-H., & Han, S.-J. (1997). Organic carbon, calcium carbonate, and clay mineral distributions in the Korea Strait region, the southern part of the East Sea. *Journal of the Korean Society of Oceanography* (in Korean) 32, 128–137.

Kim, D., Choi, M.-S., Oh, H.-Y., Song Y.-H., Noh, J.-H., & Kim, K.H. (2011). Seasonal export fluxes of particulate organic carbon from $^{234}Th/^{238}U$ disequilibrium measurements in the Ulleung Basin (Tsushima Basin) of the East Sea (Sea of Japan). *Journal of Oceanography* 67, 577–588. https://doi.org/10.1007/s10872-011-0058-8

Kim, D., Yang, E.J., Kim, K.H., Shin, C.-W., Park, J., Yoo, S., & Hyun, J.-H. (2012). Impact of an anticyclonic eddy on the summer nutrient and chlorophyll a distribution in the Ulleung Basin, East Sea (Japan Sea). *ICES Journal of Marine Science* 69, 23–29. https://doi.org/10.1093/icesjms/fsr178

Kim, K.H., & Park, N.J. (2003). Estimation of sedimentation and particle mixing rates in Ulleung Basin of the East Sea (Sea of Japan) using ^{7}Be, ^{234}Th, ^{210}Pb and ^{137}Cs. *Journal of Korean Society of Oceanography* 38, 157–165.

Kim, M., Hwang, J., Rho, T., Lee, T., Kang, D.-J., Chang, K.-I., Noh, S., Joo, H., Kwak, J.-H., Kang, C.-K., & Kim, K.-R. (2017). Biogeochemical properties of sinking particles in the southwestern part of the East Sea (Japan Sea). *Journal of Marine Systems* 167, 33–42. https://doi.org/10.1016/j.jmarsys.2016.11.001

Koo, B.-Y., Kim, S.-P., Lee, G.-S., Chung, G.S. (2014). Seafloor morphology and surface sediment distribution of the Southwestern part of Ulleung Basin, East Sea. *Journal of Earth Science Society* 35, 131–146. https://doi.org/10.5467/JKESS.2014.35.2.131

Kwak, J.H., Han, E., Hwang, J., Kim, Y.I., Lee, C.I., & Kang, C.-K. (2017). Flux and stable C and N isotope composition of sinking particles in the Ulleung Basin of the East/Japan Sea. *Deep-Sea Reseasrch II* 143, 62–72. https://doi.org/10.1016/j.dsr2.2017.03.014

Kwak, J.H., Hwang, J., Choy, E.J., Park, H.J., Kang, D.-J., Lee, T., Chang, K.-I., Kim, K.-R., & Kang, C.-K. (2013a). High primary production and f-ratio in summer in the Ulleung basin of the East/Japan Sea. *Deep-Sea Research I* 79, 74–85. https://doi.org/10.1016/j.dsr.2013.05.011

Kwak, J.H., Lee, S.H., Park, H.J., Choy, E.J., Jeong, H.D., Kim, K.R., & Kang, C.K. (2013b). Monthly measured primary and new productivities in the Ulleung Basin as a biological "hot spot" in the East/Japan Sea. *Biogeosciences* 10, 4405–4417. https://doi.org/10.5194/bg-10-4405-2013

Lee, H.J., Choug, S.K., & Yoon, S.H. (1996). Slope-stability change from late Pleistocene to Holocene in the Ulleung Basin, East Sea (Japan Sea). *Sedimentary Geology* 104, 39–51. https://doi.org/10.1016/0037-0738(95)00119-0

Lee, J.S., An, S.-U., Park, Y.-G., Kim, E., Kim, D., Kwon, J.N., Kang, D.-J., & Noh, J.-H. (2015). Rates of total oxygen uptake of sediments and benthic nutrients fluxes measured using an in situ autonomous benthic chamber in the sediment of the slope off the southwestern part of Ulleung Basin, East Sea. *Ocean Science Journal* 50(3), 581–588. https://doi.org/10.1007/s12601-015-0053-x

Lee, J.S., Kim, K.H., Shim, J., Han, J.H., Choi, Y.H., & Khang, B.-J. (2012). Massive sedimentation of fine sediment with organic matter and enhanced benthic-pelagic coupling by an artificial dyke in semi-enclosed Chonsu Bay, Korea. *Marine Pollution Bulletin* 64, 153–163. https://doi.org/10.1016/j.marpolbul.2011.09.033

Lee, S.H., Bahk, J.J., Kim, S.-P., & Park, J.-Y. (2016). Physiography and late Quaternary sedimentation. In K. I. Chang, C.-I. Zhang, C. Park, D.-J. Kang, S.-J. Ju, , S.-H. Lee, M. Wimbush (Eds.), Oceanography of the East Sea (Japan Sea) (pp. 389–414). Springer, Cham. https://doi.org/10.1007/978-3-319-22720-7

Lee, T., Hyun, J.-H., Mok, J.S., & Kim, D. (2008). Organic carbon accumulation and sulfate reduction rates in slope and basin sediments of the Ulleung Basin, East/Japan Sea. *Geo-Marine Letters* 28, 153–159. https://doi.org/10.1007/s00367-007-0097-8

Lee, T., Kim, D., Khim B.-K., & Choi, D.-L. (2010). Organic carbon cycling in Ulleung Basin sediment, East Sea. *Ocean Polar Research* (in Korean) 32, 145–156. https://doi.org/10.4217/OPR.2010.32.2.145

Lepore, K., Moran, S.B., & Smith, J.N. (2009). ^{210}Pb as a tracer of shelf-basin transport and sediment focusing in the Chukchi Sea. *Deep-Sea Research II* 56, 1305–1315. https://doi.org/10.1016/j.dsr2.2008.10.021

Liu, K.-K., Iseki, K., & Chao, S.-Y. (2000). Continental margin carbon fluxes. In R. B. Hanson, H. Ducklow, J.G. Field (Eds.), The Changing Ocean Carbon Cycle: A midterm synthesis of the Joint Global Ocean Flux Study. International Geosphere-Biosphere Programme Book Series (Vol. 5, pp. 187–239). Cambridge Univ. Press, New York.

Martens, C.S., & Klump, J.V. (1984). Biogeochemical cycling in an organic-rich coastal marine basin 4. An organic carbon budget for sediments dominated by sulfate reduction and methanogenesis. *Geochimica Cosmochimica Acta* 48, 1987–2004. https://doi.org/10.1016/0016-7037(84)90380-6

Muller-Karger, F.E., Varela, R., Thunell, R., Luerssen, R., Hu, C., & Walsh, J.J.J. (2005). The importance of continental margins in the global carbon cycle. *Geophysical Research Letters* 32, L01602, https://doi.org/10.1029/2004GL021346

Müller, P.J., & Suess, E. (1979). Productivity, sedimentation rate, and sedimentary organic matter in the oceans–I. Organic carbon preservation. *Deep-Sea Research A* 26, 1347–1362. https://doi.org/10.1016/0198-0149(79)90003-7

Park, K.-A., Ullman, D.S., Kim, K., Chung Y.J., & Kim, K.-R. (2007). Spatial and temporal variability of satellite-observed subpolar front in the East/Japan Sea. *Deep-Sea Research I* 54, 453–470. https://doi.org/10.1016/j.dsr.2006.12.010

Park, K.-A., Woo, H.-J., & Ryu, J.-H. (2012). Spatial scales of mesoscale eddies from GOCI chlorophyll-a concentration images in the East/Japan Sea. *Ocean Science Journal* 47, 347–358. https://doi.org/10.1007/s12601-012-0033-3

Rabouille, C., Caprais, J.C., Lansard, B., Crassous, P., Dedieu, K., Reyss, J.L., & Khripounoff, A. (2009). Organic matter budget in the southeast Atlantic continental margin close to the Congo Canyon: In situ measurements of sediment oxygen consumption. *Deep-Sea Research II* 56, 2223–2238. https://doi.org/10.1016/j.dsr2.2009.04.005

Reimers, C.E., Jahnke, R.A., & McCorkle, D.C. (1992). Carbon fluxes and burial rates over the continental slope and rise off central California with implications for the global carbon cycle. *Global Biogeochemical Cycles* 6, 199–224. https://doi.org/10.1029/92GB00105

Rowe, G.T., Boland, G.S., Phoel, W.C., Anderson, R.F., & Biscaye, P.E. (1994). Deep-sea floor respiration as an indication of lateral input of biogenic detritus from continental

margins. *Deep-Sea Research II* 41, 657–668. https://doi.org/10.1016/0967-0645(94)90039-6

Rowe, G.T., Morse, J., Nunnally, C., & Boland, G.S. (2008). Sediment community oxygen consumption in the deep Gulf of Mexico. *Deep-Sea Research II* 55, 2686–2691. https://doi.org/10.1016/j.dsr2.2008.07.018

Rowe, G.T., Theroux, R., Phoel, W., Quinby, H., Wilke, R., Koschoreck, D., Whitledge, T.E., Falkowski, P.G., & Fray, C. (1988). Benthic carbon budgets for the continental shelf south of New England. *Continental Shelf Research* 8, 511–527. https://doi.org/10.1016/0278-4343(88)90066-0

Sauter, E.J., Schlùter, M., & Suess, E. (2001). Organic carbon flux and remineralization in surface sediments from the northern North Atlantic derived from pore-water oxygen microprofiles. *Deep-Sea Research I* 48, 529–553. https://doi.org/10.1016/S0967-0637(00)00061-3

Schmidt, S., Howa, H., Mouret, A., Lombard, F., Anschutz, P., & Labeyrie, L. (2009). Particle fluxes and recent sediment accumulation on the Aquitanian margin of Bay of Biscay. *Continental Shelf Research* 29, 1044–1052. https://doi.org/10.1016/j.csr.2008.11.018

Smith, Jr., K.L., & Hinga, K.R. (1983). Sediment community respiration in the deep sea. In: G.T. Rowe (Eds.), The Sea (pp. 331–370). Wiley, New York.

Suess, E. (1980). Particulate organic carbon flux in the oceans-surface productivity and oxygen utilization. *Nature* 288, 260–263. https://doi.org/10.1038/288260a0

Tengberg, A., Stahl, H., Mùller, V., Arning, U., Andersson, H., & Hall, P.O.J. (2004). Intercalibration of benthic flux chambers I. Accuracy of flux measurements and influence of chamber hydrodynamics. *Progress in Oceanography* 60, 1–28. https://doi.org/10.1016/j.pocean.2003.12.001

Thomson, J., Brown, L., Nixon, S., Cool, G.T., & MacKenzie, A.B. (2000). Bioturbation and Holocene sediment accumulation fluxes in the northeast Atlantic Ocean (Benthic Boundary Layer experiment sites). *Marine Geology* 169, 21–39. https://doi.org/10.1016/S0025-3227(00)00077-3

van Weering, T.C.E., de Stigter, H.C., Boer, W., & de Hass, H. (2002). Recent sediment transport and accumulation on the NW Iberian margin. *Progress in Oceanography* 52, 349–371. https://doi.org/10.1016/S0079-6611(02)00015-0

Walsh, J.J., Premuzic, E.T., Gaffney, J.S., Rowe, G.T., Harbottle, G., Stoenner, R.W., Balsam, W.L., Betzer, P.R., & Macko, S.A. (1985). Organic storage of CO_2 on the continental slope off the mid-Atlantic bight, the southeastern Bering Sea, and Peru coast. *Deep-Sea Research A* 32, 853–883. https://doi.org/10.1016/0198-0149(85)90120-7

Walsh, J.J. (1991). Importance of continental margins in the marine biogeochemical cycling of carbon and nitrogen. *Nature* 350, 53–55. https://doi.org/10.1038/350053a0

Wenzhöfer, F., & Glud, R.N. (2002). Benthic carbon mineralization in the Atlantic: a synthesis based on in situ data from the last decade. *Deep-Sea Research I* 49, 1255–1279. https://doi.org/10.1016/S0967-0637(02)00025-0

Wollast, R. (1991). The coastal organic carbon cycle: fluxes, sources and sinks. In R.F.C. Mantoura, J.M. Martin, and R. Wollast (Eds.). Ocean Margin Processes in Global Change. Dahlem Workshop Report (pp. 365–382). Wiley Interscience, Chichester.

Yoo, S., & Park, J. (2009). Why is the southwest the most productive region of the East Sea/Sea of Japan? *Journal of Marine Systems* 78, 301–315. https://doi.org/10.1016/j.jmarsys.2009.02.014

Table 1 *Summary of Experimental Dates, Locations, Oceanographic Characteristics of the Bottom Water (Depth, Salinity, Temperature, and Dissolved Oxygen), Geomorphological Classifications, and Areas of Each Region*

Station	Date	Location	Depth	Salinity	Temperature	$O_{2\,bw}$	Region	Area
			(m)	(psu)	(°C)	(μmol dm^{-3})		(10^4 km^2)
ES–1	07/05/2014	N 35.58° E130.10°	325	34.05	0.71	217	Shelf edge–upper-slope	0.4
ES–2	13/08/2015	N35.63° E130.12°	681	34.06	0.43	193	"	
ES–3	05/05/2014	N35.67° E130.22°	950	34.06	0.23	193	Lower-slope –rise	0.7
ES–4	12/08/2015	N35.83° E130.25°	1285	34.05	0.27	180	"	
ES–5	09/05/2014	N35.92° E130.22°	1450	34.06	0.16	183	"	
ES-6	12/08/2015	N36.12° E130.42°	1670	34.05	0.22	174	Rise – basin	2.1
ES–7	20/08/2014	N37.00° E130.01°	1803	34.05	0.22	183	"	
ES–8	11/08/2015	N36.87° E130.77°	2124	34.05	0.23	173	"	
ES–9	24/08/2014	N36.99° E130.99°	2230	34.05	0.22	178	"	

Table 2 *In Situ Measurement Results of Total Oxygen Uptake Rates and Benthic Nutrients Flux*

Station	TOU	NH_4^+	$NO_2^- + NO_3^-$	PO_4^{3-}	$Si(OH)_4$
			(mmol m^{-2} d^{-1})		
ES–1	12.1†	0.10 ± 0.05	1.7 ± 0.3	0.15 ± 0.02	2.9 ± 0.5
ES–2	7.3	0.21 ± 0.02	–0.43 ± 0.08	0.028 ± 0.003	4.8 ± 0.3
ES–3	4.3	0.07 ± 0.04	–0.26 ± 0.04	0.02 ± 0.01	3.9 ± 0.7
ES–4	2.8	0.07 ± 0.01	–0.16 ± 0.03	0.024 ± 0.004	3.0 ± 0.5
ES–5	3.4	0.06 ± 0.01	-	0.018 ± 0.003	2.3 ± 0.5
ES-6	8.0†	0.05 ± 0.01	–0.25 ± 0.08	0.006 ± 0.003	7.5 ± 1.8
ES–7	2.3	-	-	0.012 ± 0.001	2.5 ± 0.9
ES–8	2.8	–0.016 ± 0.007	0.11 ± 0.02	0.035 ± 0.004	7.1 ± 1.7
ES–9	2.0	-	-	0.019 ± 0.006	2.0 ± 0.1

Note. Error denotes the uncertainty of each individual flux, estimated as the error of the slope of the concentration versus time data.

† TOU were measured by onboard incubation.

- Not determined

Table 3 *Mean OC Content (OC_∞) and the Sediment Dry Bulk Density (DBD) of Sediment at the Base of the Lowest Three Layers, Sedimentation Rate (SR)*

Station	OC_∞ (%)	DBD ($g\ cm^{-3}$)	SR ($cm\ y^{-1}$)	MAR ($g\ m^{-2}\ y^{-1}$)
ES-1	1.56 ± 0.17	1.21 ± 0.02	0.10 ± 0.02	1210 ± 243
ES-2	2.16 ± 0.01	0.40 ± 0.01	0.49 ± 0.06	1960 ± 250
ES-3	2.41 ± 0.03	0.42 ± 0.01	0.48 ± 0.04	2016 ± 178
ES-4	2.15 ± 0.01	0.44 ± 0.01	0.45 ± 0.06	1980 ± 272
ES-5	2.10 ± 0.01	0.44 ± 0.03	0.16 ± 0.01	704 ± 64
ES-6	2.09 ± 0.02	0.45 ± 0.01	0.08 ± 0.01	360 ± 46
ES-7	2.11 ± 0.01	0.45 ± 0.02	0.06 ± 0.01	270 ± 47
ES-8	1.66 ± 0.02	0.38 ± 0.01	0.06 ± 0.01	228 ± 38
ES-9	1.57 ± 0.02	0.32 ± 0.01	0.060 ± 0.001	192 ± 5

Note. The mass accumulation rates (MAR) were calculated by product DBD and SR. The errors of OC_∞ and DBD denote the standard deviation of the mean, whereas, the errors of SR were calculated using the standard errors of the slope of $^{210}Pb_{xs}$ and sediment depth. The errors of MAR were estimated from the errors of OC_∞, DBD, and SR.

Table 4 *Partitioned Organic Carbon Fluxes (Oxidation Flux (OC_{ox}), Burial Flux (OC_{burial}), Input Flux (OC_{in} = OC_{ox}+OC_{burial})), Vertical OC Flux from Water Column (J_{in}), Lateral Flux ($OC_{lat.}$), Burial Efficiency (BE = OC_{burial}/OC_{in} × 100), and Ratio of OC_{in}/J_{in} and C/N of Surface Sediment (0–1 cm)*

Station	OC_{ox}	OC_{burial}	OC_{in}	J_{in}	$OC_{lat.}$	BE	OC_{in}/J_{in}	C/N
	($g\ C\ m^{-2}\ y^{-1}$)					(%)		
ES-1	40.8	18.9 ± 4.3	59.6 ± 4.3	18.0	41.7 ± 4.3	32	3.3	8.35
ES-2	24.5	42.3 ± 5.4	66.7 ± 5.4	10.8	55.9 ± 5.4	63	6.2	8.90
ES-3	14.0	48.6 ± 4.3	62.5 ± 4.3	8.9	53.8 ± 4.3	78	7.2	8.69
ES-4	9.4	42.6 ± 5.9	51.9 ± 5.9	7.2	44.8 ± 5.9	82	7.3	8.64
ES-5	11.4	14.8 ± 1.3	26.2 ± 1.3	6.6	19.5 ± 1.3	57	3.9	8.95
ES-6	–	7.5 ± 1.0	–	6.1	–	–	–	8.91
ES-7	7.8	5.7 ± 1.0	13.5 ± 1.0	5.8	7.7 ± 1.0	42	2.3	9.01
ES-8	9.3	3.8 ± 0.6	13.1 ± 0.6	5.2	7.8 ± 0.6	29	2.5	8.95
ES-9	6.6	3.0 ± 0.1	9.6 ± 0.1	5.1	4.5 ± 0.1	31	1.9	9.07

$J_{in} = 9PP/z + 0.7PP/z^{0.5}$ (Berger et al., 1987)

Note. Uncertainties of the partitioned organic carbon fluxes were calculated by the error propagation rule.

Table 5 *Comparison of Organic Carbon Oxidation Rate, Burial Flux, and Burial Efficiency in Continental Shelf and Continental Slope Locations*

Location	Depth (m)	OC_{ox} (g C m^{-2} y^{-1})	OC_{burial} (g C m^{-2} y^{-1})	BE (%)	References
Slope off Cape Cod	50–300		1.2–2.4		Rowe et al. (1994)
Mid-Atlantic Bight	60–2000	4.8–25.6	1.1–55.2		Anderson et al. (1988; 1994), Alperin et al. (2002), DeMaster et al (2002)
Washington Slope	85–2745	0.58–2.95	3.24–25.2	12–17	Archer and Devol (1992), Hartnett and Devol (2003)
California margin	95–4078	1.0–41.8	0.2–8.8	2–49	Reimers (1992), Berelson et al. (1996)
Peru Margin	92–4902		0.2-70	7–190	Henrichs and Farrington (1984), Müller and Suess (1979), Henrichs and Farrington (1984), Betts and Holland (1991)
Northeast Atlantic Slope	1000–2000		0.12–0.24		Thomson et al. (2000)
Mexico Slope	95–3065	2.50–11.6	19.2–101.4	19–36	Hartnett et al. (2003)
Arabian Sea	300–600		0.8–21		Bhushan et al. (2001)
Congo-Angola Margin	1302–4001	5.4–13.5	1.3–4.7	30-50	Rabouille et al (2009)
Iberian Margin	104–4941	1.2–16.5	0.01-34.3	0.6-48	Epping et al. (2002), van Weering et al. (2002)
ESJ	863–2208	6.2–6.9	2.0–3.1	0.9–1.3	Lee et al. (2008; 2010)
ESJ	325–2250	6.6–40.7	1.6–25.3	16–72	This study

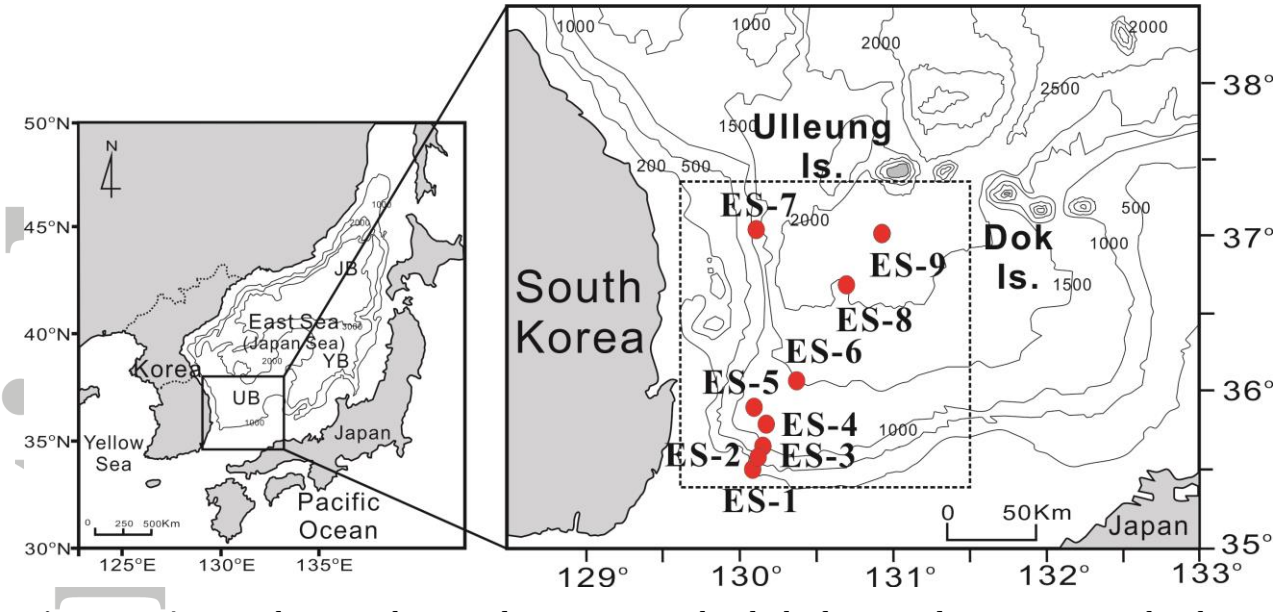

Figure 1. A map showing the sampling stations. The dashed square line represents the the study area in the southwestern part of the UB. The depth contour was drawn using the ETOPO1 dataset (**http://www.ngdc.noaa.gov/mgg/global/global.html**).

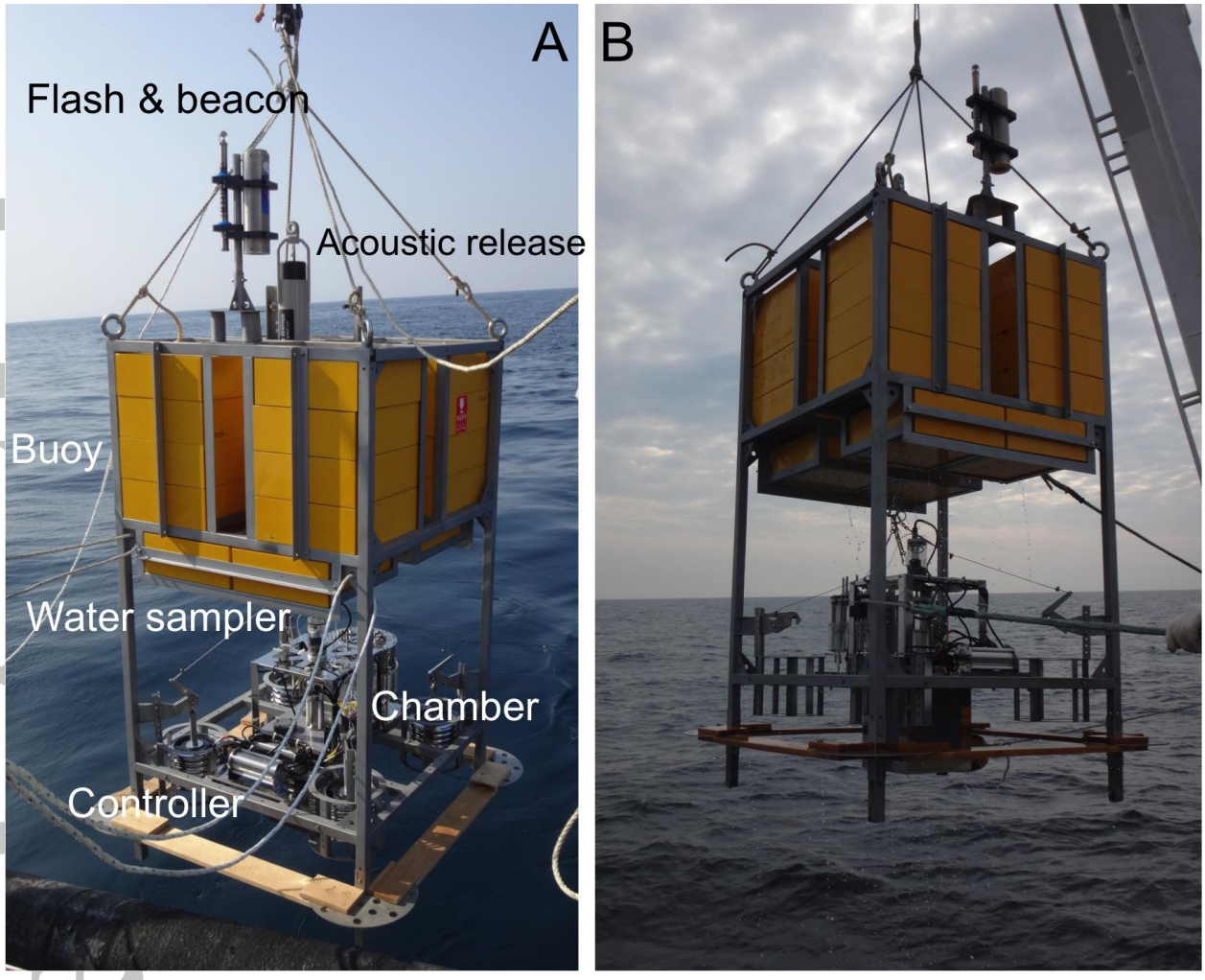

Figure 2. Pictures showing the Belc*II* deployment (A) and recovery (B) on the *Ieodo* research vessel. Belc*II* is composed of a flashlight, satellite beacon, acoustic release, buoy for deep sea, water sampler, chamber, and controller (A). The details of Belc*II* deployment and recovery are described in the Materials and Methods section.

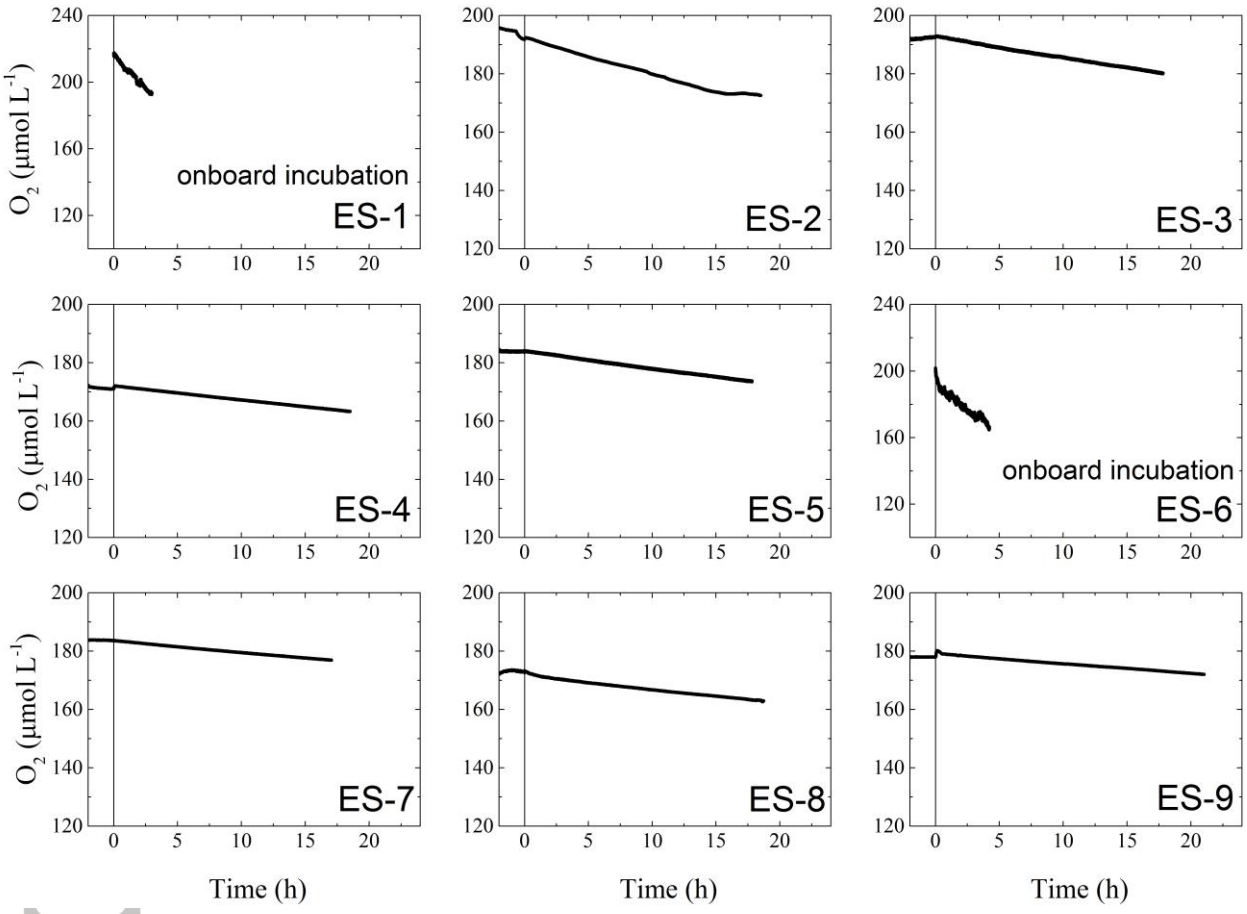

Figure 3. Evolution of O_2 with increasing time for incubation. The results of ES-1 and ES-6 are onboard measurements.

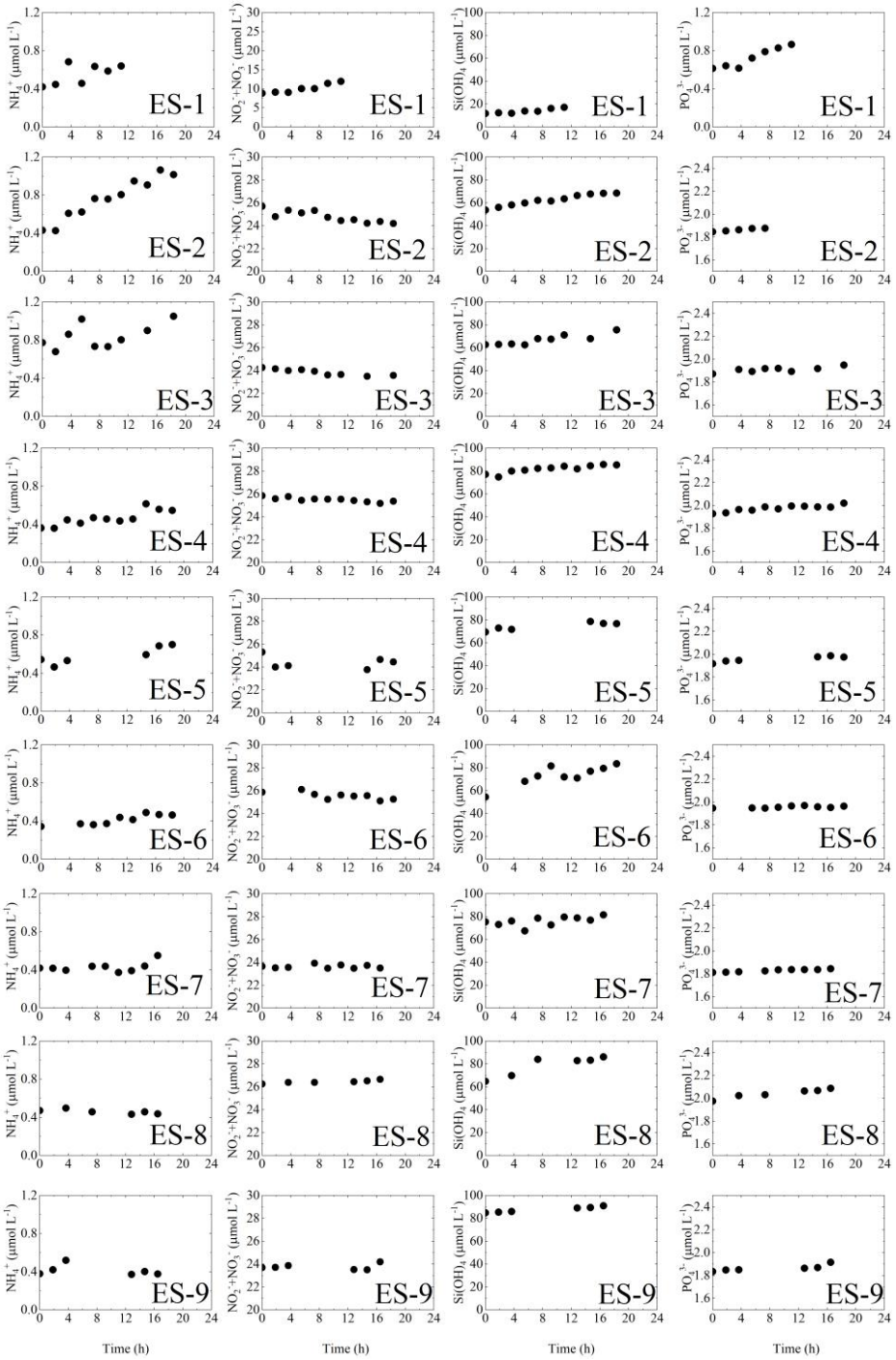

Figure 4. The evolution of ammonium, sum of nitrate (nitrate + nitrite), silicate, and phosphate concentrations during the in situ incubation.

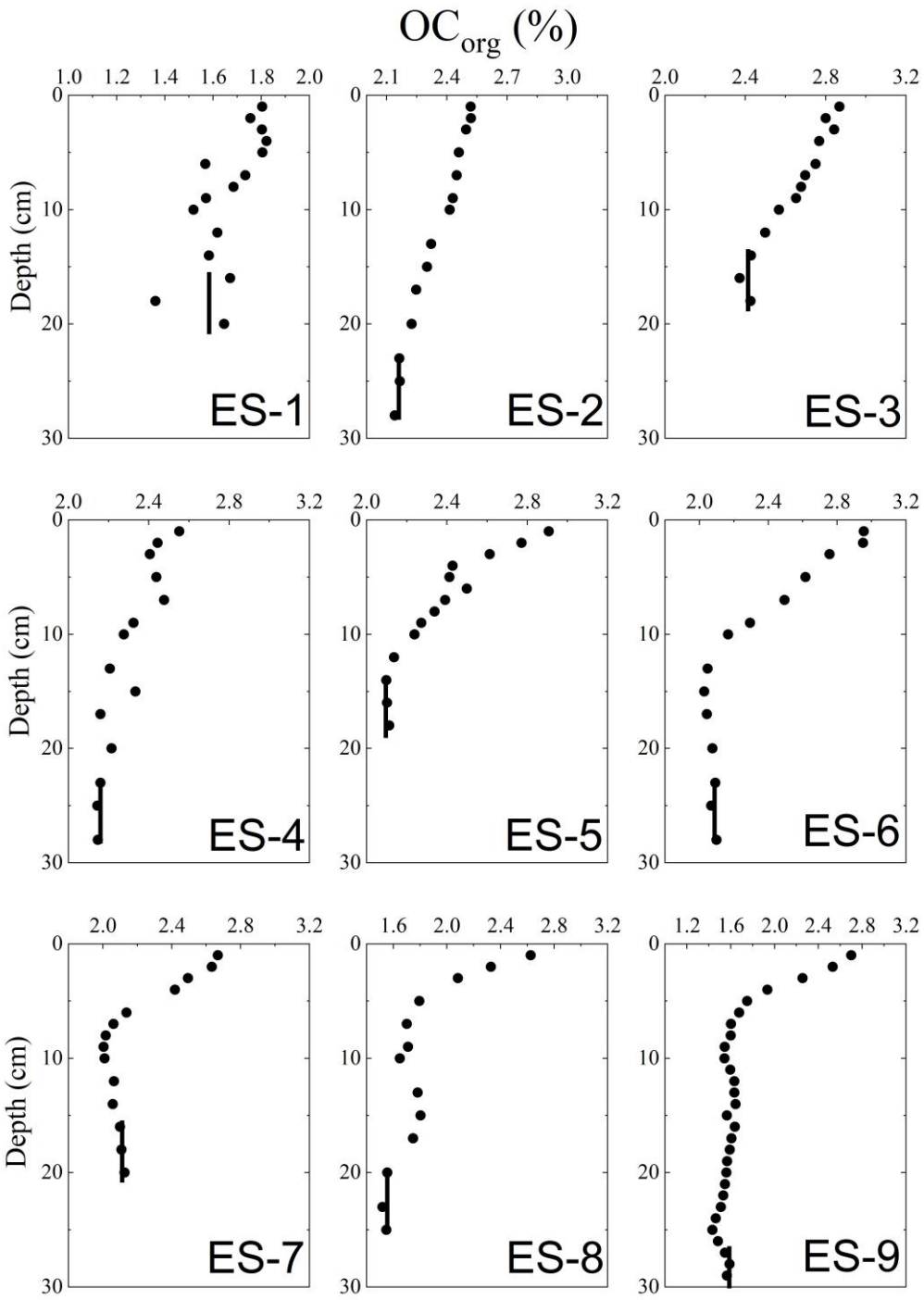

Figure 5. Vertical distribution of organic carbon contents of sediments across the slope to the basin. The solid line represents the average content at the lowest three layers of the core (OC_{∞}).

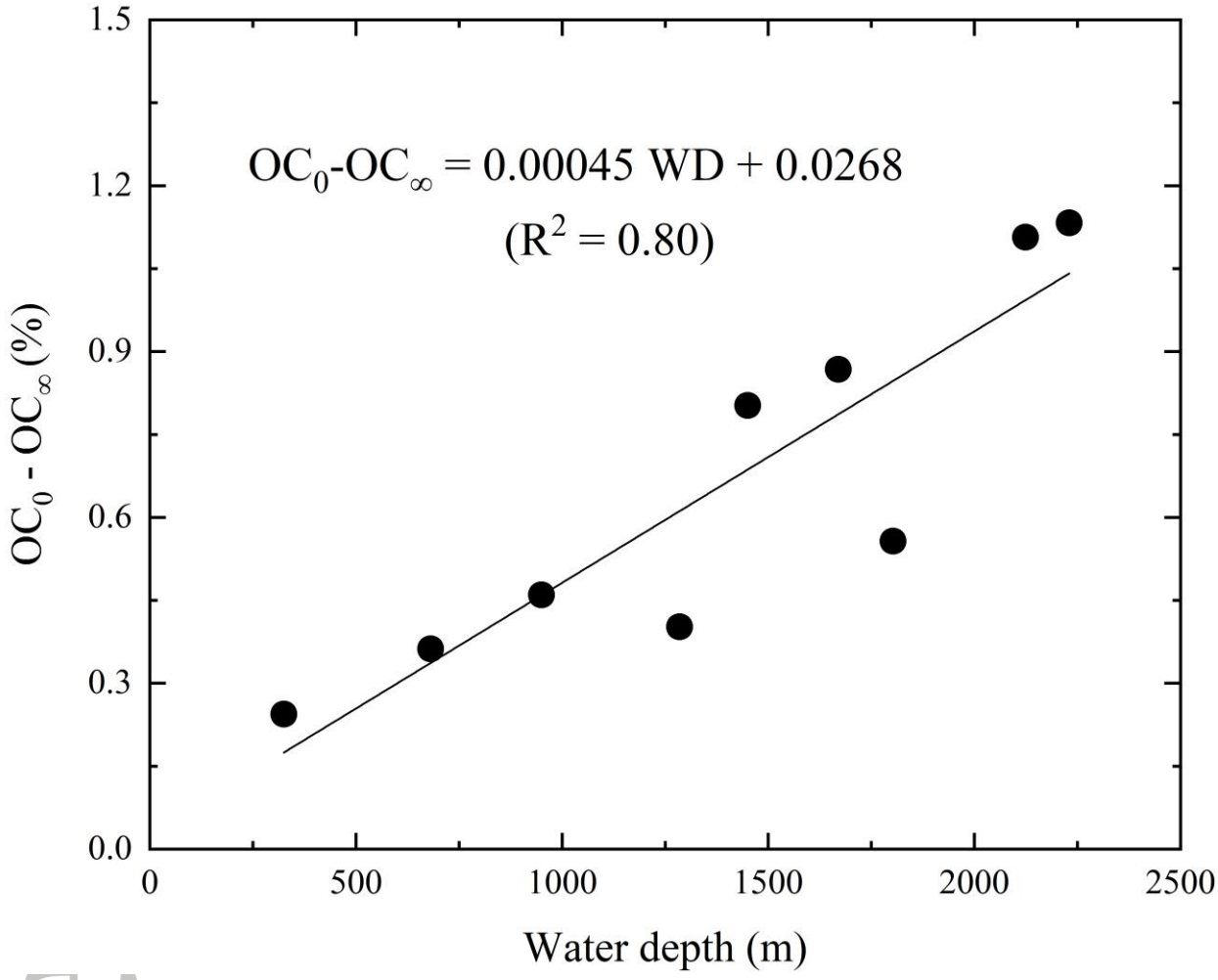

Figure 6. The relationship of water depth versus (OC_0 - OC_∞). The solid line is a best fit of a linear regression.

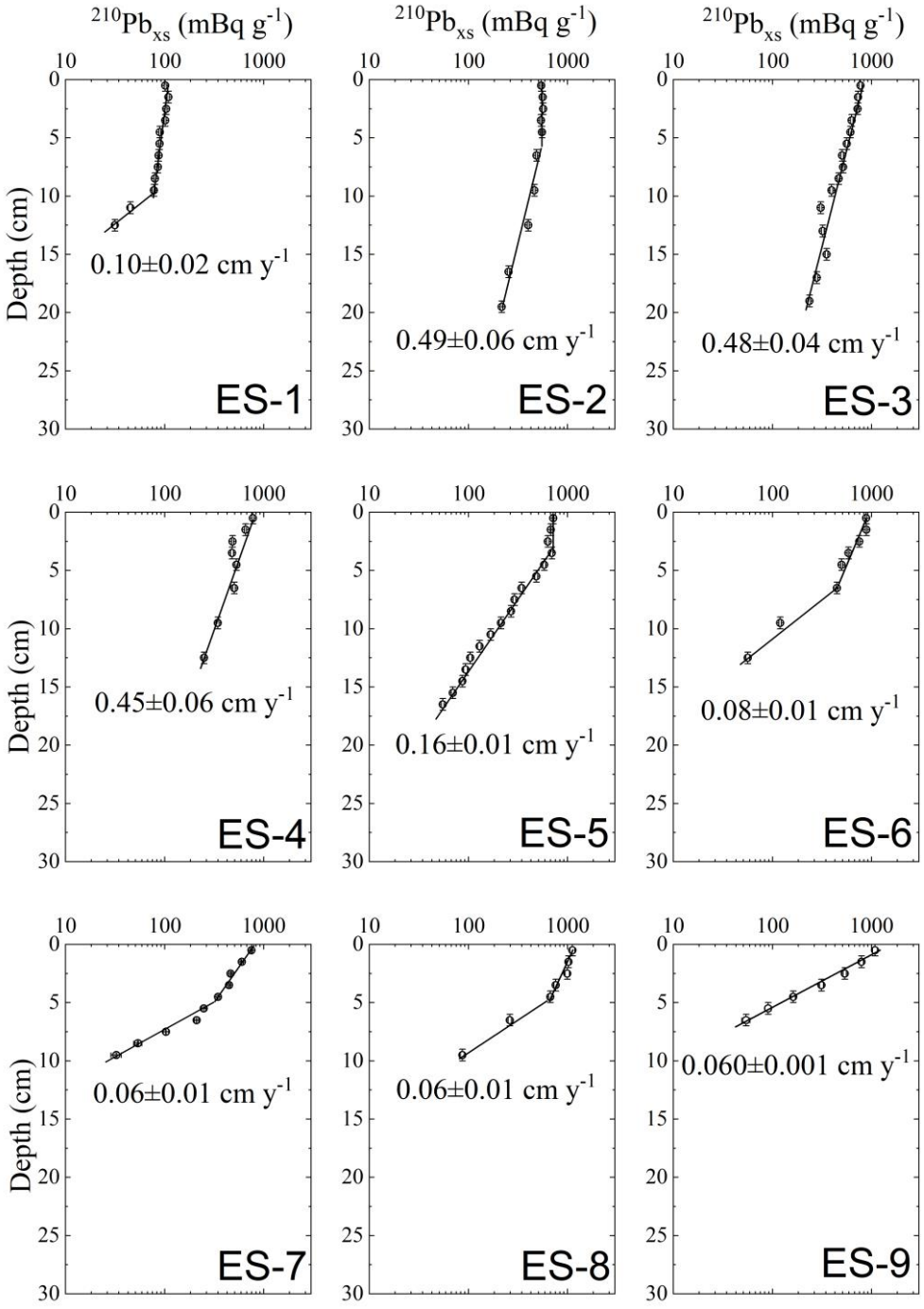

Figure 7. Vertical distribution of excess ^{210}Pb of sediments across the slope to the basin.

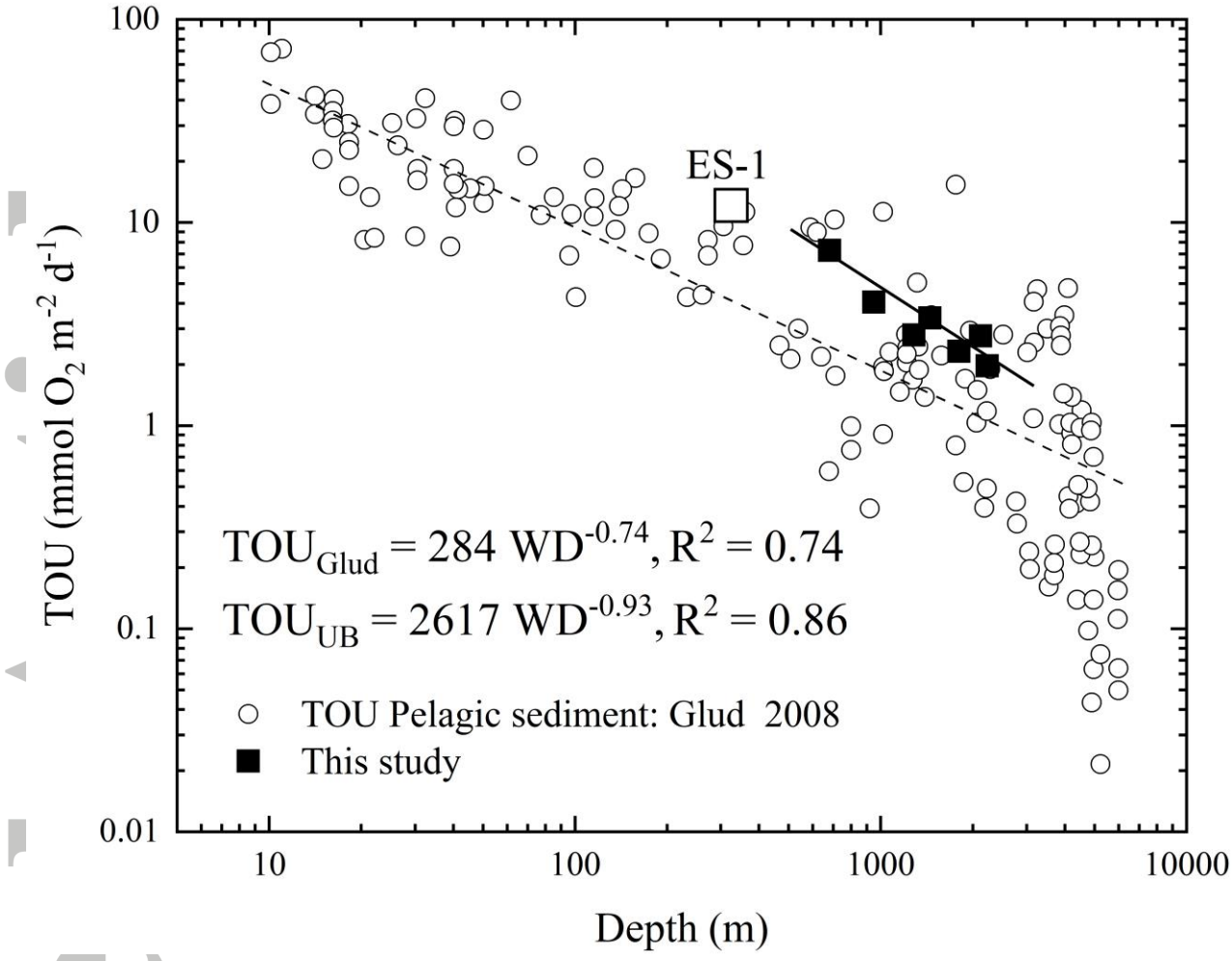

Figure 8. Comparison of the depth attenuation of TOU in the southwestern part of the UB (dark square) to the global ocean (open circle). The data set of global oceans was compiled by Glud et al. (2008), who refer to those references. The empirical relationship of UB was estimated using the in situ measurement results, which are excluded from the TOU of ES-1

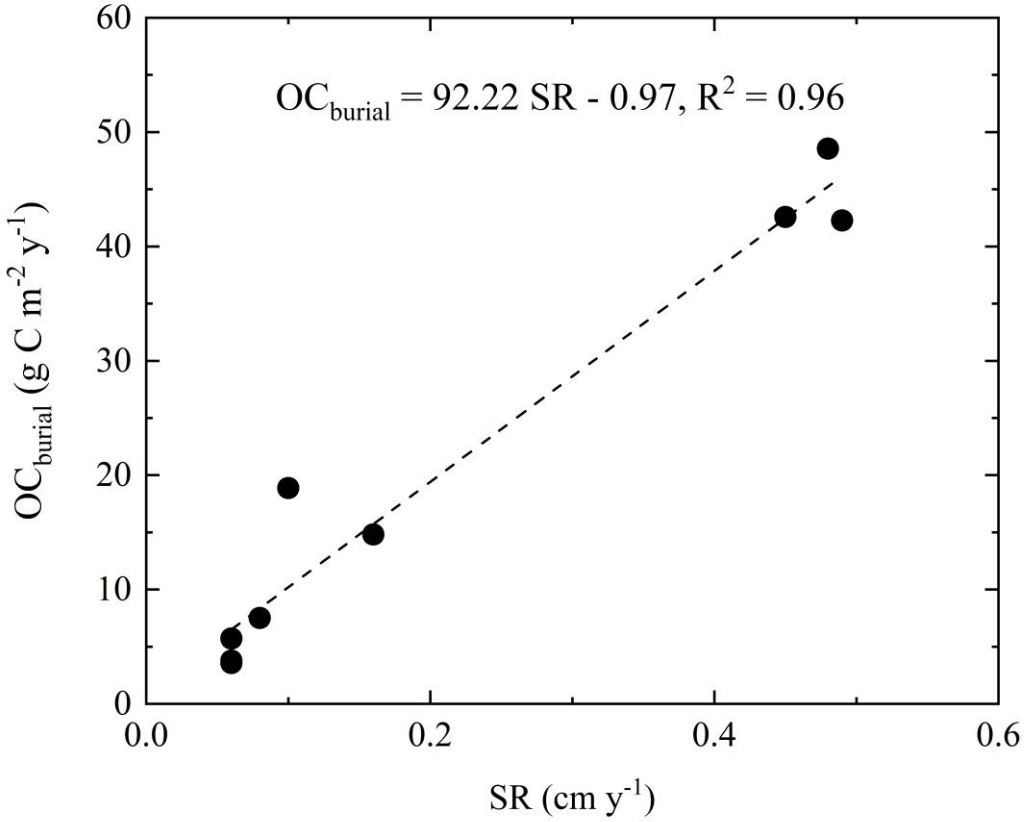

Figure 9. The relationship between the sedimentation rate and burial flux of organic carbon. The dashed line represents the linear regression result, which is OC_{burial} = 99.22SR – 0.97 (R^2 = 0.96).

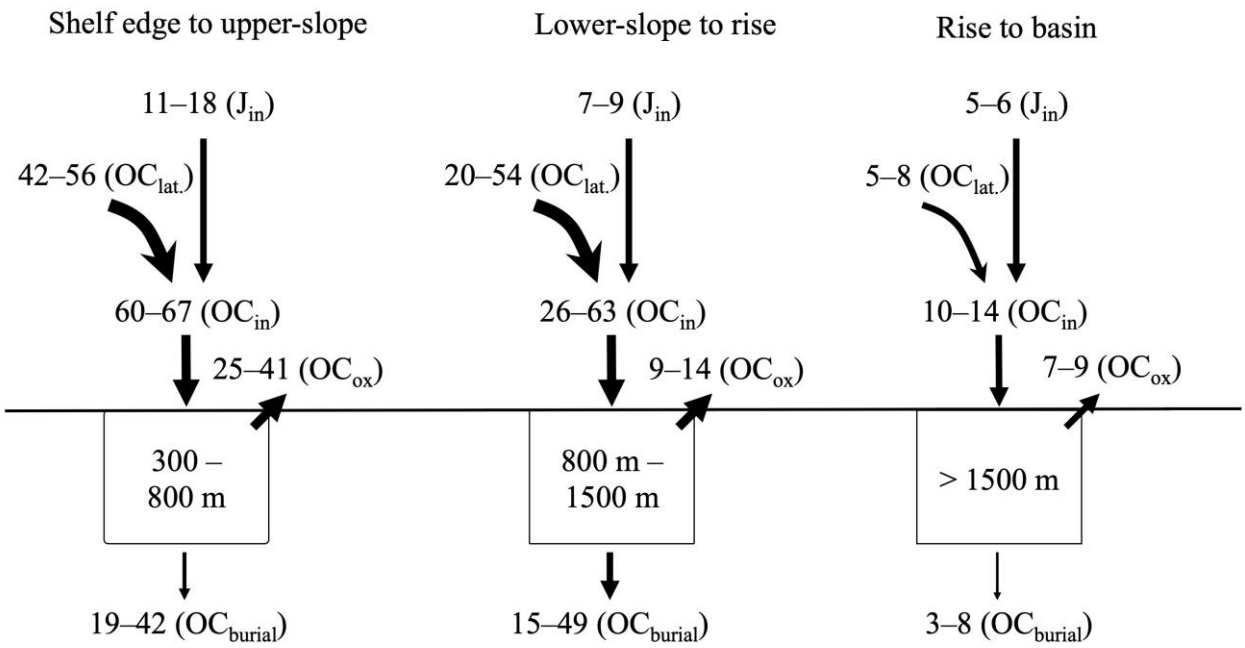

Figure 10. Organic carbon mass balance budget across the slope to the basin. The explanations of the partitioned OC fluxes, vertical flux from the water column (J_{in}), lateral flux ($OC_{lat.}$), input flux to sediment (OC_{in}), oxidation flux (OC_{ox}), and burial flux (OC_{burial}) results are given in the Discussion section.

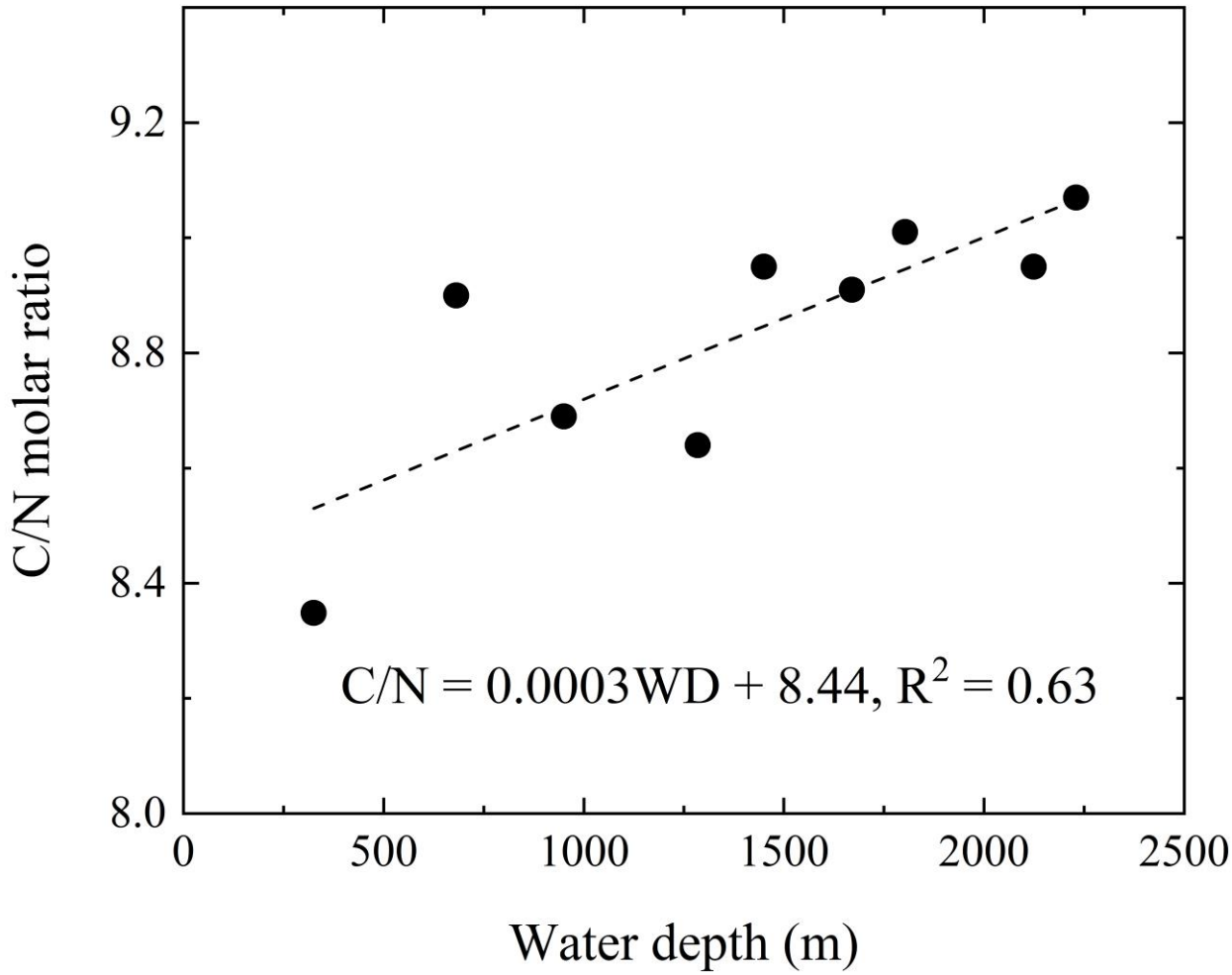

Figure 11. The linear relationship between C/N molar ratio and water depth. The linear relationship (dashed line) is C/N = 0.00003 water depth + 8.44 (R^2 = 0.63).